FABRICATION AND CHARACTERIZATION OF PIEZOELECTRIC TAPE CERAMIC FOR ELECTRIC GENERATOR

THESIS

BY

ORAPAN HEMADHULIN

A Thesis Submitted in Partial Fulfillment of Requirements for

The Master of Science Degree in Physics

Sakon Nakhon Rajabhat University

December 2019

All Rights Reserved by Sakon Nakhon Rajabhat University

FABRICATION AND CHARACTERIZATION OF PIEZOELECTRIC TAPE CERAMIC FOR ELECTRIC GENERATOR

BY

ORAPAN HEMADHULIN

A Thesis Submitted in Partial Fulfillment of Requirements for
The Master of Science Degree in Physics
Sakon Nakhon Rajabhat University
December 2019

All Rights Reserved by Sakon Nakhon Rajabhat University

THESIS APPROVAL

SAKON NAKHON RAJABHAT UNIVERSITY

FOR MASTER OF SCIENCE IN PHYSICS

Thesis Title: Fabrication and characterization of piezoelectric tape ceramic for electric generation

Author: Orapan Hemadhulin

Thesis Examination Committee

.... Chairperson
(Asst. Prof. Dr.Udom Tipparach)

.... Committee and advisor
(Dr.Hassakorn Wattanasarn)

.... Committee
(Assoc. Prof. Dr.Tosawat Seetawan)

Approval by the Curriculum Committee

....
(Dr.Hassakorn Wattanasarn)
Chair of the Committee for Curriculum
Administration Approval
Sakon Nakhon Rajabhat University

Approval by Graduate School

....
(Assoc. Prof. Dr.Sikan Pienthunyakorn)
The Director of Graduate School
Sakon Nakhon Rajabhat University

26 December 2019

Copyright of Sakorn Nakhon Rajabhat University

ACKNOWLEDGEMENTS

Firstly, I want to thank the members of thesis Advisory Committee: Dr Hassakorn Wattanasarn for their useful comment and suggestion for the work included in this thesis.

I have enjoyed working with people in the Piezoelectric Research Laboratory (PERL) Excellence on Alternative Energy (CEAE) and Program of Physics (Graduate) Faculty of Science and Technology, Sakon Nakhon Rajabhat University (SNRU) for support the research place instrument in my thesis.

Finally, I thank my beloved family whose love and encouragement are extremely to me. I appreciate what they have done for me throughout the years. With beloved ones around, I can forward full of passion and hope.

Orapan Hemadhulin

TITLE Fabrication and characterization of piezoelectric tape ceramic for electrical generator

AUTHOR Orapan Heamdhulin

ADVISOR Dr. Hassakorn Wattanasarn

DEGREE M.Sc. (Physics)

INSTITUTION Sakon Nakhon Rajabhat University

YEAR 2019

ABSTRACT

In this work, the researcher explained the characteristics of Piezoelectric tape ceramic for electricity generation of Lead zirconate titanate Strontium, Potassium Niobium, using commercial Method Composites and mixed oxide Methods. Crystal structure was studied by X-ray diffraction, dielectric constant, ferroelectric property and electricity production. It was found that composite tape ceramic. The composite shows the crystalline structure, forming a mixture of tetragonal phase and cubic phase, and the ceramic mixed oxide tape showing the crystal structure as tetragonal phase. At the same time, the dielectric constant and dielectric loss by composite method showed that the trend increased when the temperature increased and cannot check the maximum dielectric temperature maybe because of the temperature of the substance. Dielectric constant by mixed oxide and the dielectric loss is stable in high temperatures plus the temperature shift, the maximum dielectric value and also showing the ferroelectric properties of composite and mixed oxide tapes in the case of electricity production of tape ceramic, the ceramic mixed oxide tape ceramic shows the highest electrical efficiency.

Keyword Lead zirconate titanate, strontium, potassium,niobium, Tape ceramic

ชื่อเรื่อง การประดิษฐ์และอธิบายลักษณะของแผ่นเทปเซรามิกพิโซอิเล็กทริก สำหรับผลิตไฟฟ้า

ผู้วิจัย นางสาวอรพรรณ เหมะธุลิน

กรรมการที่ปรึกษา ดร. หรรษกร วรรธนะสาร

ปริญญา วท.ม. (ฟิสิกส์)

สถาบัน มหาวิทยาลัยราชภัฏสกลนคร

ปีที่พิมพ์ 2562

บทคัดย่อ

งานวิจัยนี้ผู้วิจัยได้อธิบายลักษณะของแผ่นเทปเซรามิกพิโซอิเล็กทริก สำหรับผลิตไฟฟ้า ของสารเลคเซอร์โคเนตไทเทตสตรอนเซียมโพแทสเซียมไนโอเบียมด้วยวิธีแบบคอมโพสิตและวิธีแบบมิก ออกไซด์ ได้ศึกษาโครงสร้างผลึกด้วยการเลี้ยวเบนของรังสีเอกซ์ ค่าคงที่อิเล็กทริก สมบัติเฟร์โรอิเล็กทริก ทดสอบการผลิตไฟฟ้า ผลการวิจัยพบว่า เทปเซรามิกแบบคอมโพสิตแสดงโครงสร้างผลึกเกิดเป็นโครสร้างผสมเป็นเตตระโกนอลเฟสและคิวบิคเฟส และเทปเซรามิกแบบมิกออกไซด์แสดงโครงสร้างผลึกเป็นเตระโกนอลเฟส ในขณะเดียวกันค่าคงที่ไดอิเล็กทริกและค่าการสูญเสียไดอิเล็กทริกโดยวิธีคอมโพสิตมีแนวโน้มเพิ่มขึ้นเมื่ออุณหภูมิสูงขึ้น ค่าอุณหภูมิไดอิเล็กทริกสูงสุดไม่สามารถตรวจได้ อาจจะเป็นเพราะอุณหภูมิของสาร และค่าคงที่ไดอิเล็กทริกแบบมิกออกไซด์มีค่าเพิ่มขึ้น และการสูญเสียไดอิเล็กทริกมีความเสถียรในอุณหภูมิสูง แถมเกิดการเลื่อนของอุณหภูมิค่าไดอิเล็กทริกสูงสุด และยังแสดงคุณสมบัติเฟร์โรอิเล็กทริกของเทปเซรามิกทั้งแบบคอมโพสิตและมิกออกไซด์ กรณีศึกษาการผลิตไฟฟ้าของแผ่นเทปเซรามิกพบว่าแผ่นเทปเซรามิกแบบมิกออกไซด์แสดงประสิทธิภาพไฟได้สูงที่สุด

คำสำคัญ เลคเซอร์โคเนตไทเทเนต สตรอนเซียมโพแทสเซียสไนโอเบียม
เทปเซรามิกพิโซอิเล็กทริก

TABLE OF CONTENTS

CHAPTER PAGE

1 INTRODUCTION 1

Motivation 1

Research Objectives 2

Scope and Limitation of the Thesis 3

Outcome of Thesis 3

Thesis structure 3

2 THEORY AND LITERATURE REVIEWS 5

Piezoelectric materials 5

Piezoelectric properties 8

Piezoelectric composites 10

Ferroelectric materials 14

Ferroelectric domain and hysteresis loop 15

Lead zirconate titanate (PZT) 18

Tape casting 21

Literature reviews 24

3 MATERIALS AND METHODS 28

Materials 28

Methods 29

Synthesis powder preparation of PZT-SKN 29

TABLE OF CONTENTS (continued)

CHAPTER PAGE

Synthesis powder preparation of PSKZTN 31

Synthesis slurry tape ceramic process by PZT-SKN and PSKZTN 33

Mechanical properties 35

Properties of the sample 37

Ferroelectric properties measurement 40

Piezoelectric module 44

4 RESULTS AND DISCUSSION 46

Phase structure 46

PZT-SKN powder inspection results with x-ray diffraction Technique 46

PSKZTN powder inspection results with x-ray diffraction Technique 47

The result of the binder of tape ceramic with x-ray diffraction Technique 48

The result of the of tape ceramic with x-ray diffraction technique 49

Physical properties 52

TABLE OF CONTENTS (continued)

CHAPTER PAGE

Microstructure 54

Dielectric properties 59

Ferroelectric properties 64

Piezoelectric module 67

5 CONLUSION 70

Fabricate piezoelectric ceramic tape with tape casting 70

Investigate the dielectric properties polarization ceramic tape of the hysteresis loop and the piezoelectric properties 70

study the electricity production of the ceramic tape that is prepared 71

REFERENCES 73

APPENDIX

PUBLICATIONS 78

CURRICLUM VITAE 87

LIST OF TABLES

CHAPTER PAGE

1 Functional Properties of PZT–xSKN Ceramics Sintered at 1250 °C 20

2 The chemicals source for preparation 28

3 Detail information of precursor 100 g 32

4 Composition of tape casting slurry 33

5 XRD data of the PZT-SKN and PSKZTN evaluated to the lattice parameter ***a***, ***c*** and tetragonal ***c/a***, density ($\mathrm{g\ cm^{-3}}$), Theoretical Density ($\mathrm{g\ cm^{-3}}$) relative density (%) and Vickers Hardness ($\mathrm{N\ mm^{-2}}$) 53

6 Showing the result of residual polarization (Pr), saturated polarization (Ps), the applicable electric field (E_C) and the piezoelectric coefficient (d_{33}) of the PZT-SKN tape ceramic. 65

7 Showing the result of residual polarization (Pr), saturated polarization (Ps), the applicable electric field (E_C) and the piezoelectric coefficient (d_{33}) of the PSKZTN tape ceramic 66

LIST OF FIGURES

CHAPTER PAGE

1 The perovskite structure of PZT with a cubic lattice, Centrosymmetric with zero polarization 7

2 The perovskite structure of PZT with a tetragonal lattice, Non-centrosymmetric with a net polarization 7

3 The relative of crystal structure was separate is 32 symmetry 8

4 Direct piezoelectric effect and converse piezoelectric effect 9

5 Connectivity patterns for two-phase piezocomposites 10

6 Schematic diagram of piezocomposites with 0-3 and 1-3 connectivity 11

7 The characteristic domain of normal ferroelectric 16

8 Illustrated the hysteresis loop of polarization, with dashed lines is array domain. The first process of state was array in direction arrow 17

9 Morphotropic phase boundary (left) and enhanced dielectric and piezoelectric properties (right) in the Pb(Zr,Ti)O_3 system 18

10 Doctor Blade tape casting machine 21

11 shows the hysteresis loop of (a) (1 - x) PZT-xSKN and (b) (1 - y) PZT-ySNN at sintering temperature of 1175 ° C section (c) - (f) Forced electric field values (E_c) and residual polarization (P_r) of both ceramics at different temperatures 25

LIST OF FIGURES (continued)

CHAPTER PAGE

12 SEM image (a) and specimens of bimorph specimens sintered at 1000 °C.. 26

13 The dielectric constant and dielectric loss dependent on temperature of
the PZT-0.02SKN 27

14 Chart summarizing the synthetic process PZT-SKN 30

15 The process of powder was mixed in deionized water 31

16 The formation process was carries out by uniaxial hydraulics method 32

17 Flow chart for the processing of PZT-SKN and PSKZTN 34

18 principle of x-ray diffraction analysis 35

19 Shimadzu X–Ray Diffract meter 6100 36

20 Showing X-ray source sample input characteristics and X-ray inspection
equipment 36

21 Show density Kit 37

22 Vickers hardness tester model 38

23 the scanning electron microscope techniques 39

24 Samples surface was tape ceramic 40

25 the measurement was carries out by Chen Hwa 1061 LCR–Meter 41

26 the investigate characteristics Sawyer-Tower circuits 41

27 The direction of positive polarization usually is made to coincide with the
Z-axis 42

LIST OF FIGURES (continued)

CHAPTER PAGE

28 Piezoelectric coefficient meter 43

29 Show the characteristics of Piezoelectric Modules 44

30 Measuring the electric potential difference from a change in mechanical
energy to the electric potential 45

Chapter 1

Introduction and Background

Introduction of this thesis composed of motivation, objective, scope and limitation, outcomes of the Thesis and dissertation will be presented in this chapter.

MOTIVATION

Piezoelectric devices are made from lead zirconate titanate ceramic (PZT) and are widely used in the medical, applications electric sensors and electronic industries for their exceptional piezoelectric properties. PZT is the most widely used for transducer application due to its flexibility in doping and property design, and low cost (Joseph Robert Scholz., 2009 & Fuli Zhu et al., 2015). The ceramic plate forming process can be assembled into electronic devices. There are many ways using in the screen printing and tape casting.

Tape casting is discovered in the 1940s during the second world war when there is a serious lack of quartermaster materials to produce mica capacitors. (G Helke et al., 1999; Niall J. Donnelly et al., 2007; S. Abhinay et al., 2016). Tape casting is referred to as the doctor-blade process, which the slurry is spread over a surface using a carefully controlled by a doctor blade. As a result, films of up to hundreds of meters in length and as the thickness has made than $1 \mu m$ can be obtained, and they can be as thick as 3000 μm (G.N. Howatt et al., 1947; D. Hotza et al., 1995; R.E. Mistler et al., 2000). The materials used to make electrical equipment, most are in the group of ceramics. This is because there are many good qualities. Lead zirconate titante has a perovskite structure to its crystalline phases. This structure has Pb^{+2} cations in the A-site, oxygen anions in the face centers of the unit cell, and a distribution of zirconium and titanium cations (Zr^{+4}, Ti^{+4}) on the B-site, As the material cools into the ferroelectric state, the unit cell lengthens along one axis and an off-centering of the bond lengths occurs, forming a polarization (Joseph Robert Scholz.; 2009). Lead zirconate titanate $Pb(Zr_xTi_{1-x})O_3$ doped with Sr^{+2}, K^{+1}, and Nb^{+5} (PZT-SKN) has been studied for use in multilayer actuators and transducers. The material shows high piezoelectric coefficients and permittivity values with a high Curie Temperature, combined with good thermal stability of these properties.

In this research, the research synthesized the material composition of $0.975Pb(Zr_{0.52}Ti_{0.48})O_3$-$0.025Sr(K_{0.25}Nb_{0.75})O_3$;(PZT-SKN) and mixed oxide of $Pb_{0.975}Sr_{0.02}K_{0.025}[(Zr_{0.58}Ti_{0.42})_{0.985}Nb_{0.015}]O_3$; (PSKZTN) by forming a ceramic tape casting. The microstructure of X-ray diffraction technique (XRD), measuring the dielectric properties, measuring the polarization of the hysteresis loop, the piezoelectric coefficient (d_{33}) and investigating electricity generator of the samples were carried out.

RESEARCH OBJECTIVES

1. To fabricate piezoelectric ceramic tapes with tape casting.

2. To investigate the dielectric properties polarization ceramic tapes of the hysteresis loop and the piezoelectric properties.

3. To study the electricity production of the ceramic tapes which were prepared.

SCOPE AND LIMITATION OF THE THESIS

1. Synthesis of material synthesis of $0.975Pb(Zr_{0.52}, Ti_{0.48})O_3$-$0.025Sr(K_{0.25}, Nb_{0.75})O_3$; (PZT-SKN) tape.

2. Synthesis of mixed oxides route of $Pb_{0.975}Sr_{0.02}K_{0.025}$ $[(Zr_{0.58}, Ti_{0.42})_{0.985}Nb_{0.015}]$ O_3; (PSKZTN)

3. Studying piezoelectric properties for dielectric constant and polarization of the hysteresis loop of the samples. And fabricate piezoelectric tape models.

4. Investigating the tape ceramic generate electricity from vibration.

OUTCOME OF THE THESIS

The outcomes expected in the thesis are to obtain the, dielectric properties and polarization of the hysteresis loop of PZT-SKN and PSKZTN by forming a ceramic tape casting. The result will be published in journal of materials Today: Proceedings, with title is "Fabricating piezoelectric tape of PZT-SKN".

THESIS STRUCTURE

This thesis consists of 5 chapters; Chapter 1 introduction motivation, objectives, scope, limitation, place of work and benefits of the thesis. Chapter 2 theory and literature reviews of the fundamental piezoelectric effect, history, materials and ferroelectric properties of PZT-SKN, PSKZTN and ceramic molding method with tape casting process. Chapter 3 the materials and method. Chapter 4 the results and discussion of this thesis is exhibit. Chapter 5 the conclusion and suggestion for further work are reported.

All work is carried out in the Piezoelectric Research Laboratory (PERL), in the Center of Excellence on Alternative Energy (CEAE) at Sakon Nakhon Rajabhat University, Sakon Nakhon, Thailand.

CHAPTER 2

THEORY AND LITERATURE REVIEWS

This chapter is reviewing the piezoelectric effect, ferroelectric material, perovskite structure, ferroelectric domain and hysteresis loop, lead zirconate titanate and literature reviews.

PIEZOELECTRIC MATERIALS

Piezoelectric materials exhibit intrinsic polarization and the characteristic of this state is the thermodynamically stable and reversibility of the axis of polarization under the influence of electric field. The reversibility of the polarization, and the coupling between mechanical and electrical effects are of crucial significance for the wide technological utilization of piezoelectric materials. Piezoelectric materials can be classified in to crystals, ceramics and polymers. The most well-known piezoelectric crystal is quartz SiO_2.These include lead zirconate titanate PZT $(PbZr_xTi1_{-x})O_3$, lead titanate ($PbTiO_2$), lead zirconate ($PbZrO_3$), and barium titanate ($BaTiO_3$). There are some polymeric materials which are piezoelectric and polyvinylidene fluoride is one of them (C.Z. Rosen et al., 1992 & H. Nalwa et al., 1995).

The perovskite $Pb(Zr_xTi_{1-x})O_3$ piezoelectric ceramics play a dominant role in piezoelectric materials. PZT and its related materials have been extensively investigated because of its high dielectric constant and excellent

มหาวิทยาลัยราชภัฏพระนคร

piezoelectric properties. Above a temperature known as the Curie point *T*c, these crystallites exhibit simple cubic symmetry, the elementary cell of which is shown in Figure 1. This perovskite structure of PZT consisting of a cubic structure ABO_3 with the A-cation in the middle of the cube, the B-cation in the corner and the anion in the faces. The A and B represents the large cation, such as Ba^{2+} or Pb^{2+} and medium size cation such as Ti^{4+} or Zr^{4+}. In cubic lattice structure, the cations are located at the centers of the oxygen cages with the positive and negative charge sites coincides with no dipoles. The structure is termed as centrosymmetric with zero polarization. Temperate range lower than curie point of these crystallites take on tetragonal symmetry in which the cations are shifted off the center. This creates the positive and negative charge sites with built-in electric dipoles that can be switched to certain allowed directions by the application of an electric field. The structure is noncentral symmetric with net polarization as shown in Figure 2.

In order to make these materials piezoelectrically active a process called poling is required, poling switch is the polarization vector of each domain to the crystallographic direction which is the nearest to the direction of the applied field. Once aligned, these dipoles form regions of local alignment known as Weiss domains. Application of stress (tensile or compression) to such a material will result in the separation of charges leading to a net polarization. Polarization varies directly with the applied stress and is linearly dependent. The effect is also direction dependent, the compressive and tensile stresses will generate electric fields and hence voltages of opposite polarity. If an electric field is applied, the dipoles within the domains either contract or expand (resulting in a change in the volume). Doping with conductive fillers (CB, CNTs and metals) will enhance the electrical conductivity which leads to improved poling efficiency.

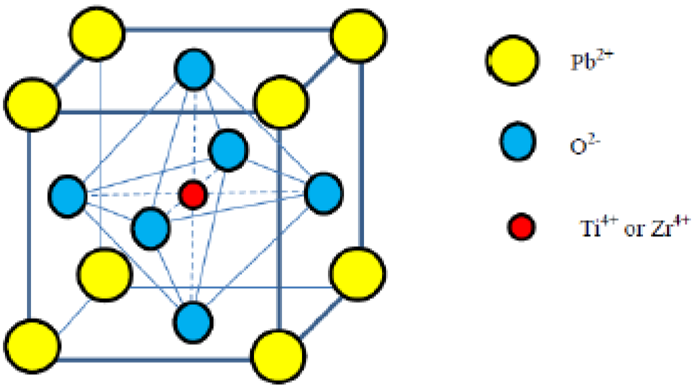
Pb^{2+}
O^{2-}
Ti^{4+} or Zr^{4+}

Figure 1 The perovskite structure of PZT with a cubic lattice, Centrosymmetric with zero polarization (Babu, et at.,2013).

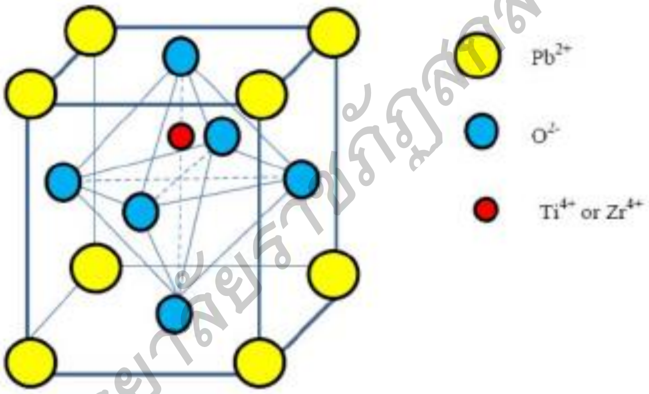
Pb^{2+}
O^{2-}
Ti^{4+} or Zr^{4+}

Figure 2 The perovskite structure of PZT with a tetragonal lattice, Non-centrosymmetric with a net polarization (Babu, et at.,2013).

PIEZOELECTRIC PROPERTIES

The piezoelectric effect discovered in 1880 BC, and initiated by the brothers Jacques and Pierre Curie. Combining their knowledge of pyroelectricity with their understanding of crystal structures and behavior, the Curie brothers demonstrated the first piezoelectric effect by using crystals of tourmaline, quartz, topaz, cane sugar, and Rochelle salt. Their initial demonstration shows that quartz and Rochelle salt exhibits the most piezoelectricity ability at the time.

The piezoelectric material is both found in nature remnants synthesized by human, it exhibits a range of piezoelectric effects. The naturally occurring of piezoelectric materials includes brilliant, cane sugar, quartz, Rochelle salt, topaz, tourmaline, and bone. The entire element above exhibiting is the Perovskite structure. Recently, the piezoelectric material is separate as 32 systems shown in Figure 3. When piezoelectric material is role under mechanical stress, a shifting of the positive and negative charge centers in the material takes place, which then results in an external electrical field. When reversed an outer electrical field either stretches or compresses the piezoelectric material as an exhibit in Figure 3.

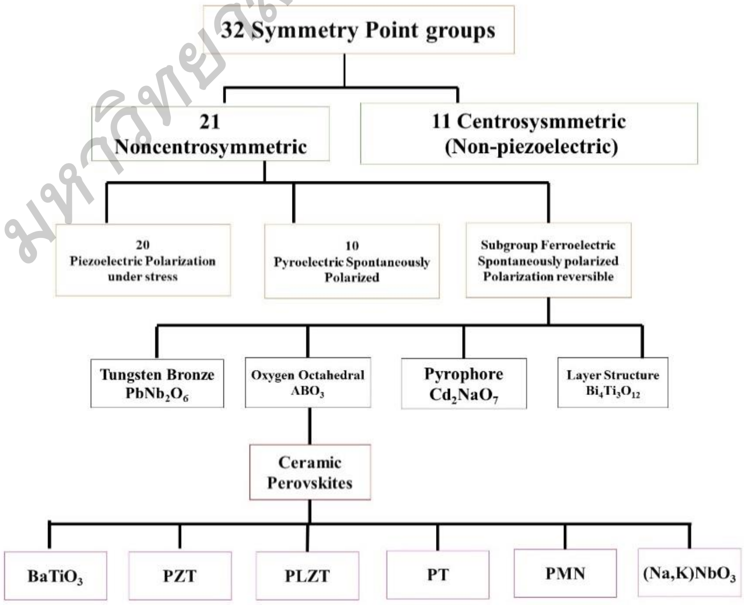
32 Symmetry Point groups
21 Noncentrosymmetric
11 Centrosysmmetric (Non-piezoelectric)
20 Piezoelectric Polarization under stress
10 Pyroelectric Spontaneously Polarized
Subgroup Ferroelectric Spontaneously polarized Polarization reversible
Tungsten Bronze $PbNb_2O_6$
Oxygen Octahedral ABO_3
Pyrophore Cd_2NaO_7
Layer Structure $Bi_4Ti_3O_{12}$
Ceramic Perovskites
$BaTiO_3$
PZT
PLZT
PT
PMN
$(Na,K)NbO_3$

Figure 3 the relative of crystal structure was separate is 32 symmetry

For the piezoelectric effect is the ability of certain materials to generate an electric charge in response due to applied mechanical stress. The word piezoelectric is derived from the Greek piezein, which means to squeeze or press, and piezo, which is Greek for “push”. The unique characteristic of the piezoelectric effect is that it is reversible, meaning that materials exhibited the direct piezoelectric effect (the generation of electricity when stress is applied) also exhibits the converse piezoelectric effect (the generation of stress when an electric field is applied) which as explained in equations (2.1) and (2.2).

Direct piezoelectric effect $$D = \varepsilon^{T} E + dT \qquad (2.1)$$

Converse piezoelectric effect $$S = S^{E} T + dE \qquad (2.2)$$

Where D is dielectric displacement, T is stress, S is strain, E s is an elastic compliance consultant under constant electric field, ε^{T} is the dielectric constant under constant stress, E and d is electric field and piezoelectric coefficient, respectively.

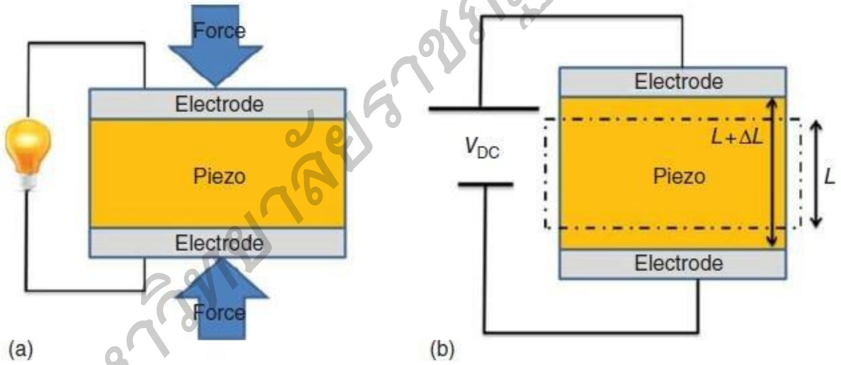

Figure 4 (a) direct piezoelectric effect (b) converse piezoelectric effect (Ali Safian and Ali Soleimani,2018)

PIEZOELECTRIC COMPOSITES

Realization of excellent properties is acquired in piezoelectric composites by the combination of its constituent phases. As a result, the demand for piezoelectric composites is growing and developing such materials is a common way to tailor the material properties for particular applications. The arrangement of the constituent phases in a composite is critical for the electromechanical coupling of the composites. The research on composite piezoelectric has been stimulated by the introduction of the concept of connectivity developed by Newnham et al. in the late 1970s [16]. Out of 10 connectivity patterns as shown in Figure 5 (0-0, 0-1, 0-2, 0-3, 1-1, 1-2, 2-2, 1-3, 2-3 and 3-3), 0-3 and 1-3 have received the most attention and is briefly described in the following sections.

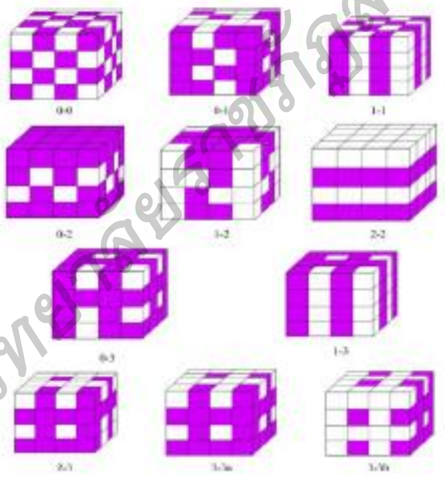

Figure 5 Connectivity patterns for two-phase piezocomposites (Babu, et at.,2013).

In this connectivity pattern, the first number denotes the physical connectivity of the active phase (ceramic) and the second number refers to the passive phase (polymer).

The simplest type is the 0-3 connectivity, in which the polymer matrix is incorporated with ceramic inclusions and 0-3 stands for the three dimensionally-connected polymer matrix filled with ceramic inclusions. Based on the connectivity patterns, various piezoelectric ceramic-polymer composites were designed and a few of them is shown in Figure 6. Of merit of these types of composites is the improved performance compared to single phase piezoceramics.

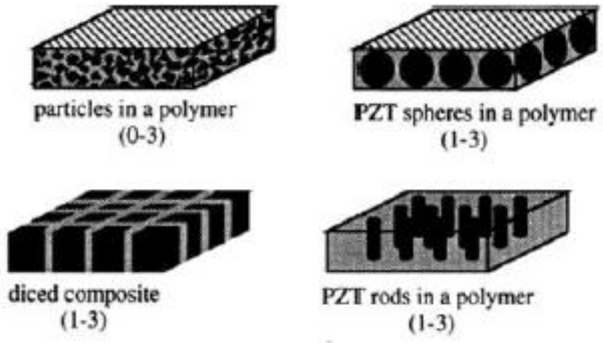

Figure 6 Schematic diagram of piezocomposites with 0-3 and 1-3 connectivity (Babu, et at.,2013).

Piezocomposites with 0-3 connectivity. The simplest type of piezocomposites is with the 0-3 connectivity, which consists of a polymer matrix incorporated with ceramic inclusions. In many ways, these types of composites is similar to polyvinylidene fluoride (PVDF). Both consists of a crystalline phase embedded in an amorphous matrix which are reasonably flexible. Polymer composites with 0-3 connectivity have several advantages over other types of composites: their ease of production, their ability for the properties to be tailored by varying the volume fraction of the ceramic inclusions and the ease of obtaining different sizes and shapes. First attempts to fabricate composites with 0-3 connectivity were made by Kitayama et al., Pauer et al. and Harrison et al. with a comparable d_{33} to PVF2 and lower dh value to that of PZT and $PVDF_2$. An improved version of these types of composite was fabricated by Banno et al. [20] using modified lead titanate incorporated in chloroprene rubber. These composites provide better piezo properties than the previous ones (Safari et al.) fabricated flexible composites with $PbTiO_3$-$BiFeO_3$ as fillers in eccogel polymer. The as-developed composites exhibit outstanding hydrostatic sensitivity. Later several researchers developed composites with 0-3 connectivity with different inclusions and these include PZT $(PbZr_xTi_{1-x})O_3$, $(PbTiO_2)$, $(PbZrO_3)$, and $BaTiO_3$ (T. Yamada et al., 1982 & T. Furukawa et al., 1979).

Piezocomposites with 1-3 connectivity. In composites with 1-3 connectivity, the ceramic rods or fibers are self-connected one dimensionally in a three dimensionally connected polymer matrix. In this type of composites, the

PZT rods or fibers are aligned in a direction parallel to the poling direction. These types of composites have relatively good hydrostatic piezoelectric constants. First attempts to fabricate composites with 1-3 connectivity were developed by Klicker et al. by incorporating PZT rods in porous polyurethane matrix. Lynn et al. also developed these types of composites by incorporating PZT rods in different types of polymer matrices. Since the high Poisson ratio of the polymer plays a negative role in the piezo properties of the composites, porous polymer matrices are used for the fabrication of 1-3 types composites. Fabrication of these types of composites is not easy and a recent study shows that the PZT particles can align in one dimension by dielectrophoretic (DEP) by applying an electric field to a composite incorporated with PZT particle (D. A. van den Ende et al., 2012)

Fabrication process. Piezoceramic materials are available in a large variety of shapes and forms. Consequently, these materials are manufactured in many different ways: sputtering, metal organic chemical vapor deposition (MOCVD), chemical solution deposition (CSD), the sol gel method and pulsed laser deposition (PLD) which is a physical method by thermal evaporation. These new technologies all techniques have (large) drawbacks. The MOCVD process has a fundamental drawback, in that the stable delivery of metal-organic precursors is difficult to achieve with conventional bubbler technology, because of the lack of suitable precursors. Moreover, precursors tent to degrade at elevated temperatures and vapor pressure in the bubbler varies with time, and therefore constant delivery is hard to achieve. The CSD method has the disadvantage that it cannot be utilized for high density memory devices because the substrate must undergo the planarization process in order to spin-coat ferroelectric films. In sol-gel methods cracks are liable to occur in the post-annealing process when the thickness of the PZT film is larger than several hundred of angstroms. Therefore, forming many thin layers of film is usually done in order to prevent cracks. However, many time repetitions of spin coating, pre-baking and post-annealing is time consuming and also increases the probability of contamination (S. B. Krupanidhi et al., 1983; M. Toyama et al., 1994; S. Jeong et al., 2003 & J.S. Zhao et al., 2004).

The major ingredient in PZT is lead oxide, which is a hazardous material with a relatively high vapor pressure at calcining temperatures. Consequently, last decades PZT also attracted attention from an environmental perspective. Concerns about the lead compound in PZT, which can during calcination and sintering release volatiles causing pollution. More concern is about the recycling and disposal of devices containing PZT, especially those used in consumers products. Extensive effort in research has been made to arrive with alternatives for PZT, which do not contain lead such as $BaTiO_3$, $Na_{0.5}Bi_{0.5}TiO_3$, $K_{0.5}Bi_{0.5}TiO_3$, $Na_{0.5}K_{0.5}NbO_3$ and many more (E.A. Gurdal et al., 2011). However, till today, none of the alternatives encounters better performance as compared to PZT for ferroelectric and piezoelectric properties (converting very efficient electrical energy into mechanical energy or vice versa).

FERROELECTRIC MATERIALS

All ferroelectric materials are perovskite, however, all polycrystalline materials are ferroelectric. Bellow a transition temperature called the Curie temperature ferroelectric and pyroelectric materials are polar and possess a spontaneous polarization or electric dipole moment. However, this polarity can be reoriented or reversed fully or in part through the application of an electric field with ferroelectric materials. Complete reversal of the spontaneous polarization is called “switching”.

The non-polar phase encountered above the Curie temperature is known as the paraelectric phase. The direction of the spontaneous polarization conforms to the crystal symmetry of the material. While the reorientation of the spontaneous polarization is a result of atomic displacements. The magnitude of the spontaneous polarization is greatest at temperatures well below the Curie temperature and approaches zero as the Curie temperature is nearing. The crystal structure is shown piezoelectric properties were separates as 20 groups, which can be spontaneous polarization with 10 groups. The spontaneous polarization is a dipole moment per volume with perpendicular to axis polarization. The generality of axis polarization parallel with crystal structure, even crystal has a dipole show piezoelectric effect. Thus, crystal of axis single dipole is exhibited spontaneous polarization. The general of spontaneous polarization cannot directly measurement from surface crystal. Since the charge was compensated from various factors. The spontaneous polarization of crystal has ion positive and negative, with ion in some temperature range within site stable, well is low free energy and center of ion positive not connect ion negative.

FERROELECTRIC DOMAIN AND HYSTERESIS LOOP

A ferroelectric material in general is defined by the existence of a permanent spontaneous polarization P_s at temperatures below the Curie temperature whereby the direction of P_s can be reversed by the application of an electric field exceeding the coercive field E_c. The value of E_c is defined using the hysteresis loop which can be recorded during a poling cycle ramping up and down the applied electric field. Theoretical calculations of the value of E_c failed up to now. A ferroelectric material is by nature always piezoelectric and also pyroelectric. A ferroelectric domain is an area of oriented spontaneous polarization. Local poling, i.e. the controlled formation of domains, makes of ferroelectrics very important materials for applications such as data storage devices or optical frequency converters. The controlled formation of domains is therefore of major importance. In general, local poling is performed by locally applying an electric field surpassing E_c using structured electrodes, named electric field poling (EFP). We investigated a new technique for controlled domain formation thereby defining the domain pattern by UV-laser light irradiation. Another technique under investigation for local poling consists in the application of an electric field with the help of a scanning probe microscope tip, named tip-based domain formation. A ferroelectric domain is an area of oriented spontaneous polarization. Local poling, i.e. the controlled formation of domains, makes of ferroelectrics very important materials for applications such as data storage devices or optical frequency converters. The controlled formation of domains is therefore of major importance. In general, local poling is performed by locally applying an electric field surpassing E_c using structured electrodes, named electric field poling (EFP). We investigated a new technique for controlled domain formation thereby defining the domain pattern by UV-laser light irradiation. Another technique under investigation for local poling consists in the application of an electric field with the help of a scanning probe microscope tip, named tip-based domain formation (G.N. Howatt et al., 1947).

In the crystal of ferroelectric material is characteristic polarization with nearby, and domain have same direction is called Ferroelectric Domain. Which have may be the single domain or multiple domains, and the junction of between domains is called Domain Wall. But when is applied electric field to cause shift of domain wall to have single domain. And then crystal receive electric field can be switching polarization in domain is called domain switching. For the crystal of normal ferroelectric will as size domain rang at micrometer and characteristic domain exhibiting in Figure 7.

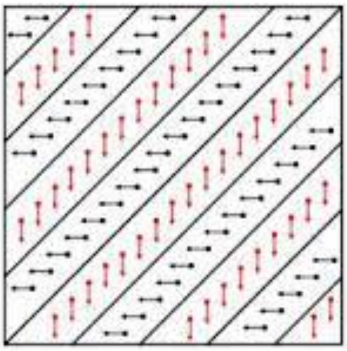

Figure 7 The characteristic domain of normal ferroelectric.

The various between crystal ferroelectric and pyroelectric, which ferroelectric can be switch dependent on direction of the applied electric field. The domain switching is investigated by hysteresis loop. The ferroelectric is characteristic hysteresis loop graph exhibited in Figure 5. When intensity of electric field with increase in direction positive, domain is exert to array in direction of electric field. The maximum of change domain will make a high polarization is called point saturated polarization. And break has electric field with the polarization decrease but not zero. Since, some domain is stability the polarization in direction positive, it makes remnant polarization. When the electric field to increase in direction negative to polarization with decrease, and intensity of electric field is making the polarization amount as zero is called coercive field (E_C). The electric field is more than E_C to be the domain switching, become characteristic is hysteresis loop. By the remnant polarization, saturated polarization and coercive field of normal ferroelectric is any high value.

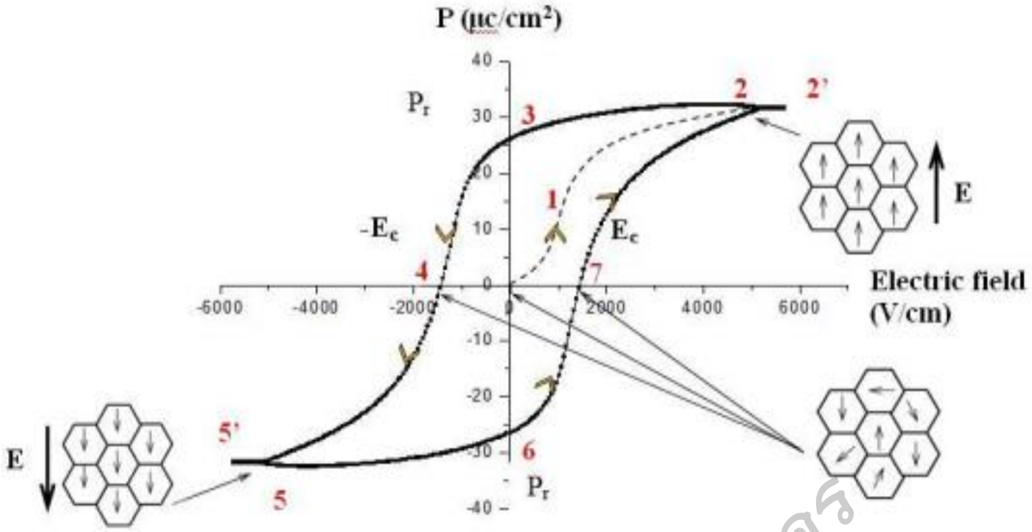
P (μc/cm²)
40
30
20
10
0
-10
-20
-30
-40
Pr
3
2
2'
E
1
Ec
-Ec
4
7
Electric field (V/cm)
-6000
-4000
-2000
0
2000
4000
6000
5'
5
6
Pr
E

Figure 8 Illustrated the hysteresis loop of polarization, with dashed lines is array domain. The first process of state was array in direction arrow. (Chunmanus Uthaisar., 2013)

LEAD ZIRCONATE TITANATE (PZT)

Lead zirconate titanate (PZT) ceramics are a solid solution of $PbZrO_3$ and $PbTiO_3$ of the formula $Pb(Zr_xTi_{1-x})O_3$. Mixtures of the compositions of atoms should only occur if the mixing does not increase the free energy of the system. The phase diagram for PZT is shown in Figure 9. At high temperatures the material is paraelectric and cubic (Pm3m). The ferroelectric phase is divided into tetragonal (P4mm) and rhombohedral (R3m) phases, with a narrow region between these two phases called a morphotropic phase boundary (MPB). The boundary defines a structural change with variation in composition that is almost temperature independent. The piezoelectric properties are enhanced near the morphotropic phase boundary between the tetragonal and rhombohedral phases, because this composition allows for spontaneous polarization in 14 different directions. Domains are easily reoriented between these directions, so properties are enhanced. In recent years, there is evidence that a monoclinic phase can also co-exist in the MPB region. But there is uncertainty around these observations and no domain structures are consistent with the habit planes required for monoclinic phase. Local and global symmetries of complex domain patterns confuse the exact structural nature of the MPB.

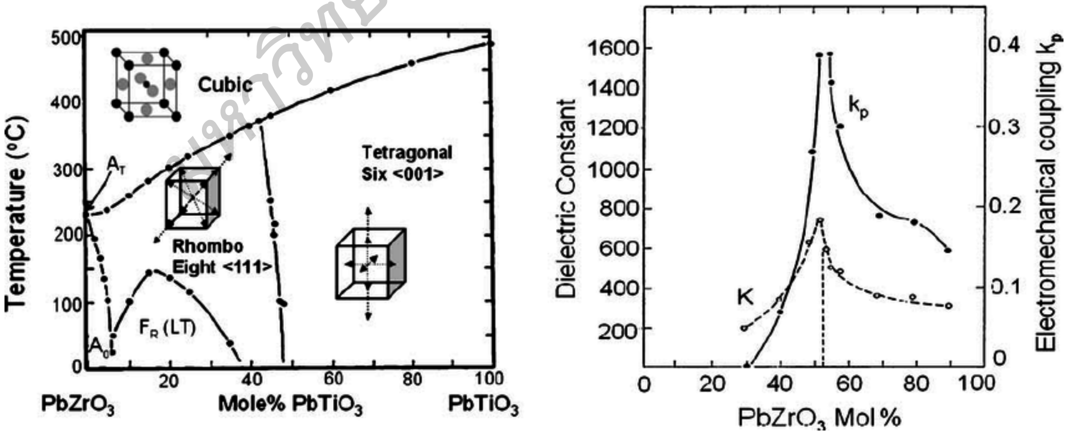

Figure 9 Morphotropic phase boundary (left) and enhanced dielectric and piezoelectric properties (right) in the $Pb(Zr,Ti)O_3$ system.
(Thomas R. Shrout et al., 2007).

$PbZr_xTi_{1-x}O_3$ (PZT) is a well-known commercially-used perovskite ferroelectric material. Key compositions with optimised piezoelectric coefficients lie at the morphotropic phase boundary (MBP, x= 0.52) between rhombohedral and tetragonal phases. Table 1 show some recent PZT based compositions using strontium potassium niobate (SKN) as a dopant in comparison with some classic formulations and d_{33} vs T_C of well-established PZT, respectively. The optimum low field value of d_{33} is 510 pC/m^{-1} for a TC = 356°C. The exceptional combination of d_{33} vs TC demonstrated by SKN doped compositions illustrates the difficulty in replacing PZT with PbO-free compositions.

Table 1 Functional Properties of PZT–xSKN Ceramics Sintered at 1250 °C

Mol. (SKN)	Grain size (mm)	T_c (°C)	$\varepsilon_{\max}$ (1 kHz)	$\varepsilon_{(50°C)}$ (1 kHz)	$tan\delta_{(50°C)}$ (1 kHz)	$d_{33}^{(High)}$ (pC/N^{-1})	$d_{33}^{(low)}$ (pC/N^{-1})	K_p
0.01	11.47 ± 2.9	375	54 000	1300	0.018	668	445	0.53
0.02	6.2 ± 2.0	356	40 200	1400	0.018	779	510	0.59
0.03	2.8 ± 1.0	341	31 100	1430	0.020	713	495	0.58
0.04	1.5 ± 0.5	323	22 600	1500	0.023	651	470	0.55
0.05	1.5 ± 0.5	305	15 300	0.025	0.025	547	395	0.47
0.03 (24h)	2.8 ± 1.0	341	40 300	1420	0.022	768	530	0.62
0.05 (24h)	1.2 ± 1.4	305	17 300	1460	0.029	559	460	0.52
PZT-6%Sr[1]	-	328	-	1300	0.004	-	289	0.58
PZT-	-	365	-	1700	.02	-	374	0.60
PZT-5A	-	365	-	1700	-	-	410	0.60

TAPE CASTING

Tape casting is first introduced in the 1940s during the second world war when there is a serious lack of quartermaster materials to produce mica capacitors (G.N. Howatt et al., 1947).In tape casting process, sometimes referred to as the doctor-blade technique, the slurry is spread over a surface using a carefully controlled blade referred to as a doctor blade. As a result, films of up to hundreds of meters in length and as thin as 1 μm technique can be obtained, and they can be thick as 3000 μm (D. Hotza et al., 1995; R.E. Mistler et al., 2000; M. Rahaman et al., 2006; G.N. Howatt et al., 2006). showed in Figure 7

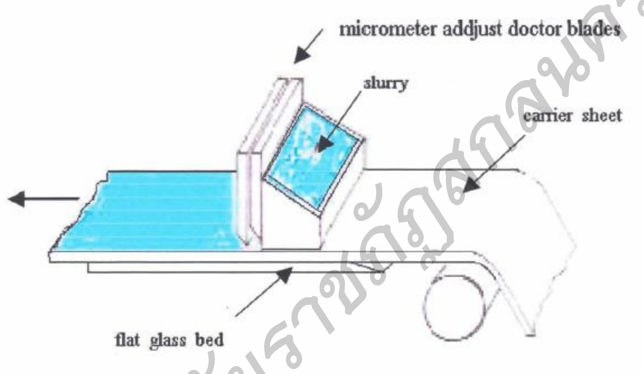

Figure 10 Doctor Blade tape casting machine (Clark & McColum, 1988)

Typical Organic additives

1. The solvent is used to temporarily make the system more fluid. The binder, which is usually an organic chemical in solid form, and ordinarily dissolved in this solvent. The ceramic powder itself is not commonly dissolved, but instead it is put into the form of an “unstable suspension” (often called* a “slip”) allowing easy flow. At a later stage in the process, the solvent is evaporated out of the system (“dried”), so it is really just a temporary material, used mostly for fluidizing. Note that the solvent fluidizes both the powder, which is not dissolved, and the binder, which usually is dissolved.

Water is the most commonly used solvent in ceramic technology. The main advantages of water are that it is cheap and safe. Water also has disadvantages, such as a tendency to chemically react with certain ceramic powders like barium titanate or aluminum nitride, degrading their properties. Also, water sometimes causes the slip to be too “viscous” (sometime referred to as too “thick”). In addition, water does not evaporate as quickly as some organic solvent, and therefore drying is much slower and requires more heating. (Shanefield et al., 1995).

For these reasons, organic solvents are often used instead of water. A typical example id toluene, which if flammable and also is suspected of being toxic. Obviously, then, the choice of solvent involves a trade off between several advantages and disadvantages.

As mentioned above, the binder and some other components are usually dissolved in the solvent. Some binders will dissolve only in water, and some others only in non-water (“nonaqueous”) liquids such as toluene. The initial choice of the solvent therefore dictates the choice of chemical family for the other additives, also. In general, the whole field of organic additives for ceramics can be divided conveniently into two categories of aqueous and nonaqueous chemical systems.

2. Dispersants. These materials, sometimes called “deflocculants” or “surfactant,” are put into the composition for two main reasons: (1) to keep the powder-solvent slip from becoming too “viscous” (having too much resistance to flow), and (2) to prevent “agglomeration” (lumpiness). The use of a powerful dispersant such as a polyacrylate can provide a reasonably low viscosity, even when only small amounts of solvent are used. Also, freedom from the lumpiness of agglomerates will usually prevent large pores from being present in the material, which is another very critical consideration. Although dispersant represent only about 8% of the current market value of the total usage of organic additives in the ceramics industry, this particular niche of the market is growing fast, because increased automation is requiring better reproducibility, and the newer dispersant are able to prevent the type of random variation in density that is caused by agglomerates.

3. Binder. After the ceramic shape (“body”) has been molded and the solvent has been evaporated, the binder is provided considerable strength, even before firing. Thus the unfired green body is strong enough to be handled for inspection and for loading into the furnace. In some cases it can be machined

on a lathe or drilled with precise holes, as is typically done with spark plug insulators, for example. Binders represent the largest segment of the current market for organic additives in ceramic processing.

4. Plasticizers. Plasticizer is a material such as ball clay which can provide plastic flow when it is wetted with water. The word is still sometimes used in that sense, but there is also another meaning. When this word is used in modern chemical technology, it means a liquid that can be added to the binder composition to prevent brittleness in the dry body. If the binder is prevented from becoming brittle when it is dried, then it is effectively stronger, and the formulator can use less of it and still achieve a practical level of unfired green strength. An example of a plasticizer is glycerin, which is excellent for use with a polyvinyl alcohol binder.

5. Others. Several categories of organic additives such as release agents, antifoams, and biocides, which are of less importance, will be covered in later sections. However, those discussions will be more understandable after some further theoretical principles have been presented.

Of course, all of the organic materials briefly described above become “burned out” or else are evaporated out of the ceramic composition by the time firing step is finished. This is one of the main advantages of organic versus inorganic additives, in addition to the designed by synthesizing chemists.

LITERATURE REVIWES

Several researches show ferroelectric properties which are reported as followings.

S.Abhinay et al. (2015) Studied powder 0.5Ba $(Zr_{0.2}Ti_{0.8})O_3$-0.5 $(Ba_{0.7}Ca_{0.3})TiO_3$ (BZT-0.5BCT) using tape casting method the distribution of the powder depends on the particle size. 1000 °C calcine powder with an input particle size range of 0.27-0.5 μm. Useful for tape casting preparation. The sediment viscosity and sedimentation height are confirmed. 1% phosphate ester by sufficient weight for the dispersing efficiency of BZT-0.5BCT to get a stable solution the role of fastener (PVB) on the tape lubricant flow properties and the properties of the BZT-0.5BCT tape has been studied. Changes in PVB content indicate that PVB must be at least 3% by weight or can be added up to 3.5% of PVB (binders) which can withstand 65% load. Different shrinkage in During the burning Relative density and piezoelectric coefficient continuously reduced with a decrease in solid loads It is observed that the temperature has a significant effect, which is able to modify the micro and electrical properties of ceramics. The highest density (94% of the true density and dielectric constant (172 pC / N^{-1}) for tapes with 3% PVB and dry weight 65% after burning at 1500 ° C / 4 hrs. The high stress (0.23%) obtained from experiments for the best surfaces show the sensor's potential.

Zhu et al. (Zhu, Qiu, Ji, Zhu, & Wen, 2015) studied potassium (K +) and sodium (Na +) substitution (1 - x) Pb $(Zr_{0.53}, Ti_{0.47})O_3$. - xSr $(K_{0.25}, Nb_{0.75})O_3$ (PZT-SKN) using Calcium 850 ° C, the best sintering temperature is 1175 ° C and (1 -y) Pb $(Zr_{0.53}, Ti_{0.47})O_3$ - ySr $(Na_{0.25}, Nb_{0.75})O_3$ (PZT-SNN), Calcination temperature 1000 ° C, the best sintering temperature is 1175 ° C (x = y = 0.005, 0.01, 0.02, 0.03, 0.04 and 0.05) When considering the structure of ABO_3 for SKN, both Sr and K are in position A. At the same time, Nb lives in the position. B because of the compensation capacitor One charge of K$^+$ and Nb5$^+$ creates half the oxygen gap. And the half gap, respectively. The SNN system is the same, while the SKN result will cause gap in the PZT by 1 in 4. This situation can also occur with SNN for polarization studies. Session of PZT – SKN / PZT – SNN From the loop, the hysteresis becomes more square shaped when increasing the amount of SKN / SNN. Grain size also decreases by increasing the amount of SKN / SNN which leads to increased grain boundary. Can occur in the ceramic system for PZT-SKN at x = 0.01 with the value of 40.65 μC cm-2 and PZT-SNN at x = 0.02 with the value of 39.81 μC cm^{-2} as shown in Figure 11.

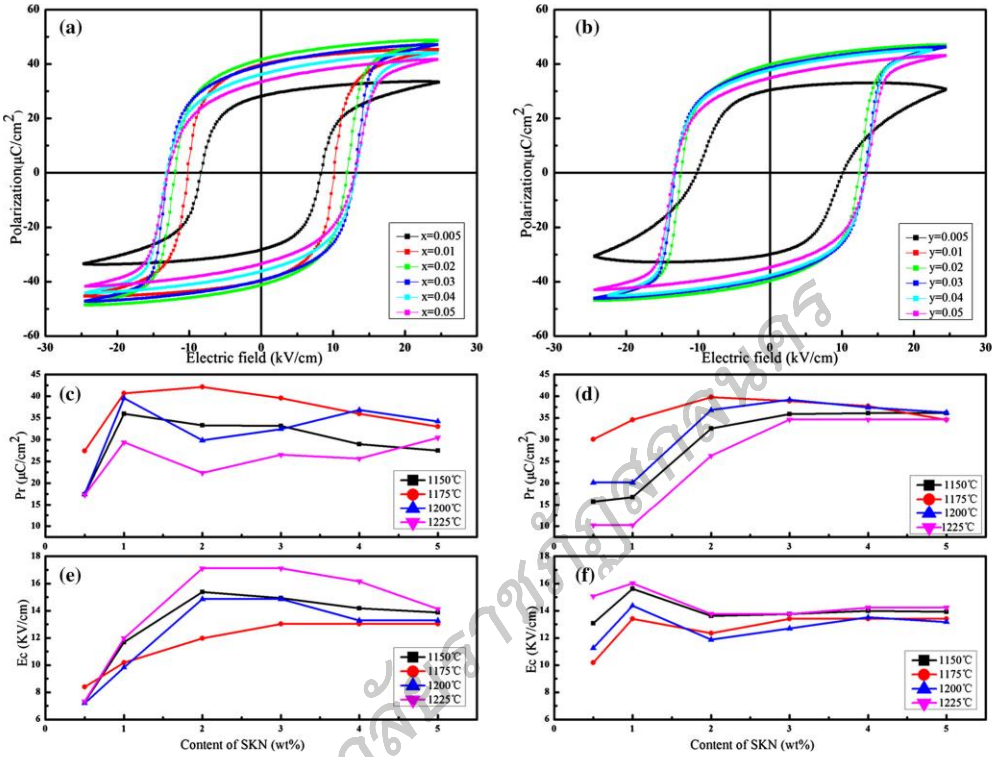

Figure 11 The hysteresis loop of (a) (1 - x) PZT-xSKN and (b) (1 - y) PZT-ySNN at sintering temperature of 1175 ° C section (c) - (f) Forced electric field values (E_c) and residual polarization (P_r) of both ceramics at different temperatures (Zhu, Qiu, Ji, Zhu, and Wen, 2015).

Chao et al. (2012). Fabrication Pb (Zr_xTi_y) O_3 - Pb $(Zn_{1/3}Nb_{2/3})$ O_3-Pb $(Ni_{1/3}Nb_{2/3})$ O_3 (PZT-PZN-PNN) by technique tape casting is a piezoelectric device. By sintering at 1000 °C for 4 hours. The tape measures 44.95 x 7.15 x 0.245 mm^3 with silver pint on both sides. Then sintered at 850 °C for 3 hours as shown in Figure 12 and then polled at 350 °C for 30 minutes under the electric field 1 KV mm^{-1}, showing displacement at 1683 mm when given Potential difference 180 V

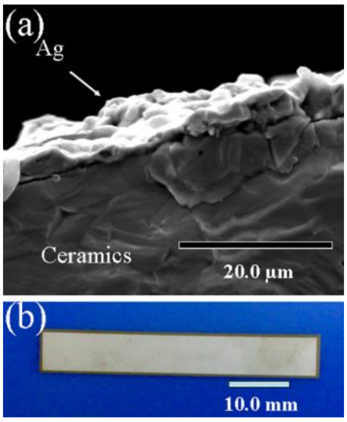

Figure 12 SEM image (a) and specimens of bimorph specimens sintered at 1000 °C (Chao, Yang, Pan, and Yang, 2012).

Niall J. Donnelly et al (2007). Studied the effect of increasing the theoretical complexity of Sr $(K_{0.25}\ Nb_{0.75})O_3$ to PZT (53/47). Example of SKN addition at 0.02 and 0.03 by sintering at 1250 °C. It was found that at 0.02SKN, the piezoelectric properties were high. As illustrated in Figure 13, it shows the PZT-0.02SKN dielectric measurement by measuring frequencies at 1, 10 and 100 kHz. The rapid increase in contact loss at temperatures above 400 °C with low frequencies is characteristic of dc. The loss of the PZT ceramic is in this range from the dielectric constant graph. And dielectric loss (Some people call the relative condition). Compare 3 frequencies which are 1, 10, 100 KHz. Found that the frequency does not spread. Coherent Which is one of the properties of Piezoelectric. The maximum dielectric constant is 470 °C.

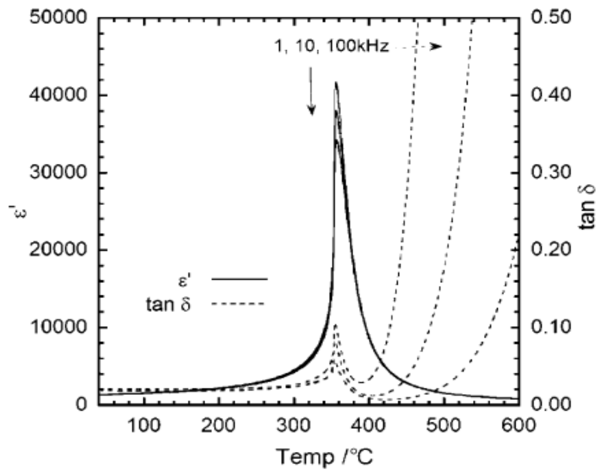

Figure 13 The dielectric constant and dielectric loss dependent on temperature of the PZT-0.02SKN

Helki et al. (Helke, Seifert, & Cho, 1999) studied Pb materials (Zr$_{0.52}$, Ti$_{0.48}$) O$_3$-Sr (K$_{0.25}$, Nb$_{0.75}$) O$_3$; (PZT-SKN). It was first reported by has good properties for fabrication as multi-layered piezoelectric actuators. The sintering of this PZT-SKN material requires temperatures up to 1250 ° C and therefore has reduced the sintering temperature. To prevent vapor evaporation and co-firing with low-melting electrodes is called low temperature co-fired ceramic (LTCC) by adding materials in the range The presence of liquid phase phases such as LiBiO$_2$ and CuO (LBC) while using the sintering temperature for LBC materials can reduce the sintering temperature of PZT.

CHAPTER 3

MATERIALS AND METHODS

This chapter presents the proviso detail of synthesizing and fabricating of PZT-SKN, PSKZTN tape. The characterized on crystal structure, density, dielectric, ferroelectric and piezoelectric property of the ceramic tape.

MATERIALS

In this study, chemicals used in the synthesis of ceramic tape, PZT-SKN and PSKZTN, are shown in Table 2.

Table 2 The chemicals source for preparation

Material name	Company	Purity
Lead oxide (PbO)	Dechen chemical co., ltd	99.00%
Zirconium dioxide (ZrO_2)	Dechen chemical co., ltd	99.00%
Titanium dioxide (TiO_2)	Dechen chemical co., ltd	99.00%
Strontium carbonate ($SrCO_3$)	Dechen chemical co., ltd	99.00%
Potassium carbonate (K_2CO_3)	Safefy technique elucidation	99.00%
Niobium oxide (Nb_2O_5)	-	99.00%

Material name	Company	Purity
Methyl Ethyl Ketone (MEK)	Biotecll and scientiflc.co.ltd	-
Ethanol	Biotecll and scientiflc.co.ltd	95.00%
Polyvinyl Butyral (PVB)	Biotecll and scientiflc.co.ltd	-
Polyethylene Glycol (PEG)	Biotecll and scientiflc.co.ltd	-
Defoamer	-	-
Phosphate	-	-
Acetone	-	99.50%
Silver Pen	-	-
DI water	-	99.95%

METHODS

1. Synthesis powder preparation of PZT-SKN

The ratio of the raw materials of PbO, ZrO_2, TiO_2, $SrCO_3$, K_2CO_3, and Nb_2O_5 has been calculated following equation;

$$PbO + ZrO_2 + TiO_2 + SrCO_3 + K_2CO_3 + Nb_2O_5 \text{ ---> } 0.975Pb(Zr_{0.52}, Ti_{0.48})O_3\text{-}0.025Sr(K_{0.025}, Nb_{0.75})O_3 \quad (3.1)$$

The PZT-SKN polar composite ceramics were prepared $0.975Pb(Zr_{0.52}, Ti_{0.48})O_3$ and $0.025Sr(K_{0.25}, Nb_{0.75})O_3$ were synthesized separately through a solid-state reaction technique. These starting materials were mixed by balling in dewater for 24 h, dried and calcined in air. The calcination conditions of the $0.975Pb(Zr_{0.52}, Ti_{0.48})O_3$ and $0.025Sr(K_{0.25}, Nb_{0.75})O_3$ were 850 °C for 4 h. The resynthesized $0.975Pb(Zr_{0.52}, Ti_{0.48})O_3$ and $0.025Sr(K_{0.25}, Nb_{0.75})O_3$ powders were subsequently mixed in stoichiometric ration, ball-milled and dried again.

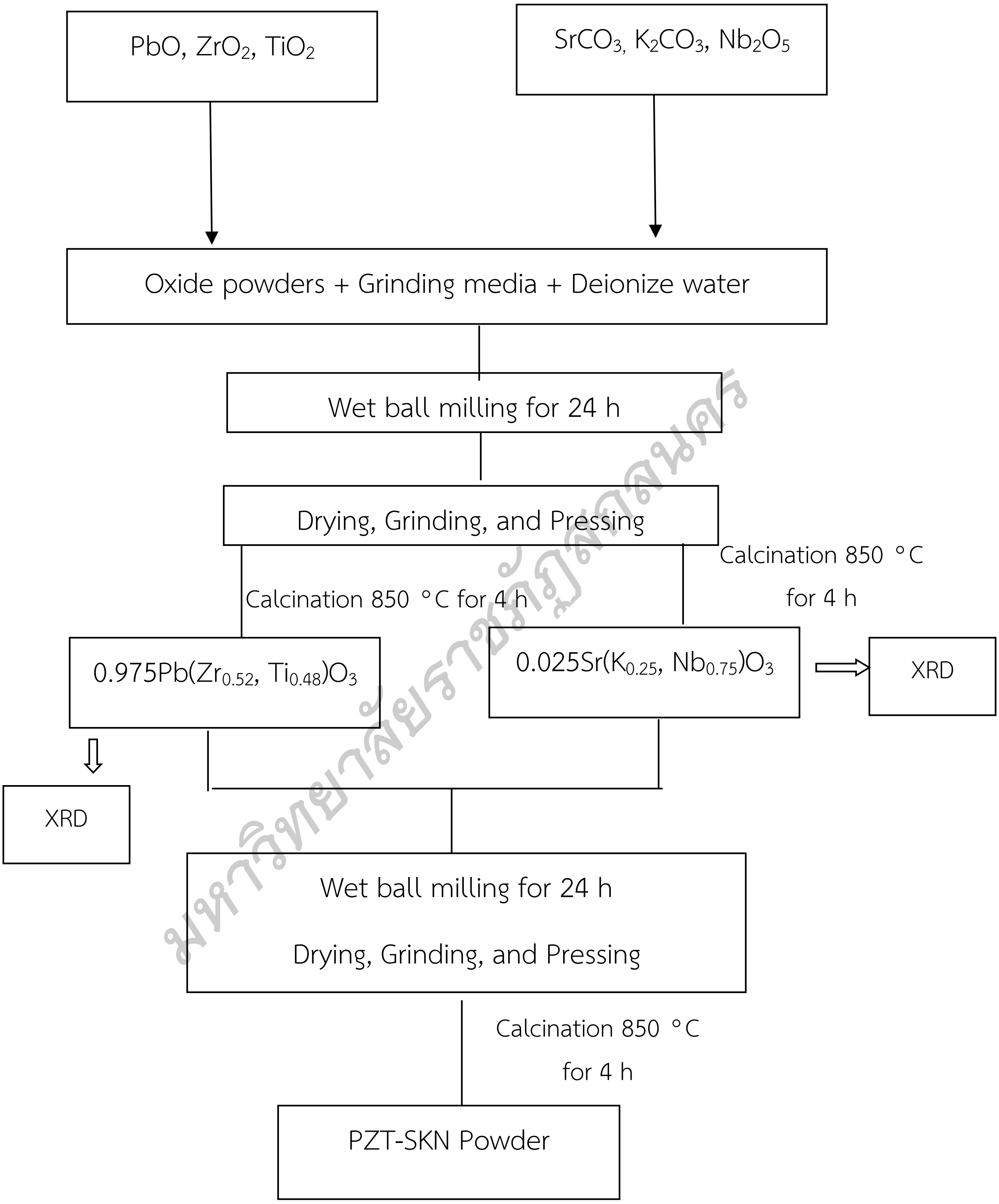
PbO, ZrO$_2$, TiO$_2$
SrCO$_3$, K$_2$CO$_3$, Nb$_2$O$_5$
Oxide powders + Grinding media + Deionize water
Wet ball milling for 24 h
Drying, Grinding, and Pressing
Calcination 850 °C for 4 h
Calcination 850 °C for 4 h
0.975Pb(Zr$_{0.52}$, Ti$_{0.48}$)O$_3$
0.025Sr(K$_{0.25}$, Nb$_{0.75}$)O$_3$
XRD
XRD
Wet ball milling for 24 h
Drying, Grinding, and Pressing
Calcination 850 °C for 4 h
PZT-SKN Powder

Figure 14 Chart summarizing the synthetic process PZT-SKN.

2. Synthesis powder preparation of PSKZTN

The raw materials of PbO, ZrO_2, TiO_2, $SrCO_3$, K_2CO_3, and Nb_2O_5 has been calculated the ratio to follow as equation;

$$PbO + ZrO_2 + TiO_2 + SrCO_3 + K_2CO_3 + Nb_2O_5 \dashrightarrow Pb_{0.975}Sr_{0.02}K_{0.025}[(Zr_{0.58,}Ti_{0.42})_{0.985}Nb_{0.015}]O_{3;} \quad (3.2)$$

The synthesized of PSKZTN were prepared by solid-state reaction. In preparation procedures, we used the raw materials of solid state reaction are weighted according to the stoichiometric ratio for raw materials. Example powders were mixed under deionized water by zirconia ball-milled for 24 h, and dried at 100 °C, crushed in an agate mortar.

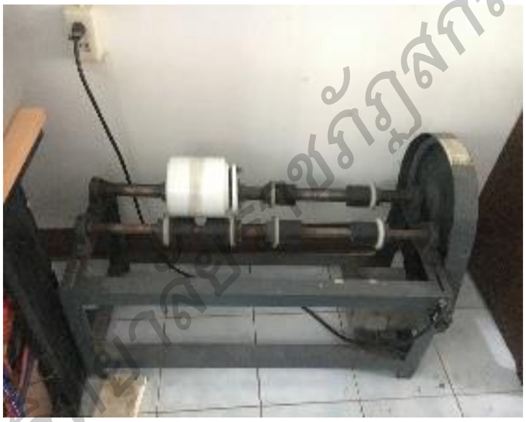

Figure 15 The process of powder was mixed in deionized water.

Table 3 Detail information of precursor 100 g.

	Precursor	Quantity		Precursor	Quantity
Composite	0.975PZT	58.3333 g	Mixed Oxide	PbO	69.5795 g
				ZrO_2	21.6415 g
				TiO_2	10.2573 g
	0.025SKN	41.6667 g		$SrCO_3$,	0.9076 g
				K_2CO_3	0.1062 g
				Nb_2O_5	0.6128 g
	Sum	100.0003 g		sum	103.0051 g

The powders were mixing formation samples with uniaxially pressed in to pellets with 10 mm in diameter and 1.3 mm in thickness under 190 MP pressures. After that, calcination was performed at 850 °C for 4 h.

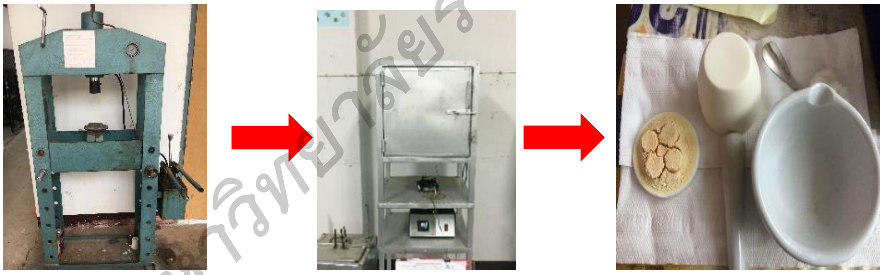

Figure 16 The formation process was carries out by uniaxial hydraulics method.

3. The synthesis slurry to tape ceramic process by PZT–SKN and PSKZTN

Typical PZT-SKN slurry was made as per the composition given in Table 3. The preparation of slurry for tape casting was carried out in two stages. In the first phase, mixture of methyl ethyl ketone (MEK), ethanol and phosphate ester hey were ball milled for 24 h in polyethylene jar using ZrO_2 balls as grinding media. and in the second stage binding system consisted of binder (polyvinyl butyral, PVB) and plasticizers (polyethylene glycol, PEG). In both the cases, they were ball milled for 6 h in polyethylene jar using ZrO_2 balls as grinding media. After mixing by ball milling, wire mesh filter slurry, then vacuum the pump out with a vacuum pump (Ax─2000 Vacuum Mixer). Then the slurry was cast in a laboratory tape caster with the stationary reservoir. A casting speed of 1.20 mms/s was maintained in all cases and left for drying. Square dimensional sample (2×2 cm^2) were cut from the green tapes. Then bake at a temperature of 100─200 °C for 1 h., leave to room temperature. Then burn binder with a temperature of 350─750 °C. leave it for 2 hours and leave to room temperature. The final sintering using the sintering temperature of 1100 ° C, the temperature dropped to room temperature for 2 h. and then leave. After examining the dielectric properties of 1─100 kHz and temperature range 30─600 ° C, examination of Ferroelectric Properties by study of hysteresis loop, the polling at room temperature for 10 min using a voltage of 2.5 kV mm^{-1} and measurement of piezoelectric coefficient.

Table 4 Composition of tape casting slurry.

Ingredient	Function	Weight (%)
Powder	Ceramic	65
Phosphate Ester	Dispersant	1
Methyl Ethyl Ketone +Ethanol	Solvent	26
Polyvinyl Butyral	Binder	4
Polyethylene Glycol	Plasticizer	3

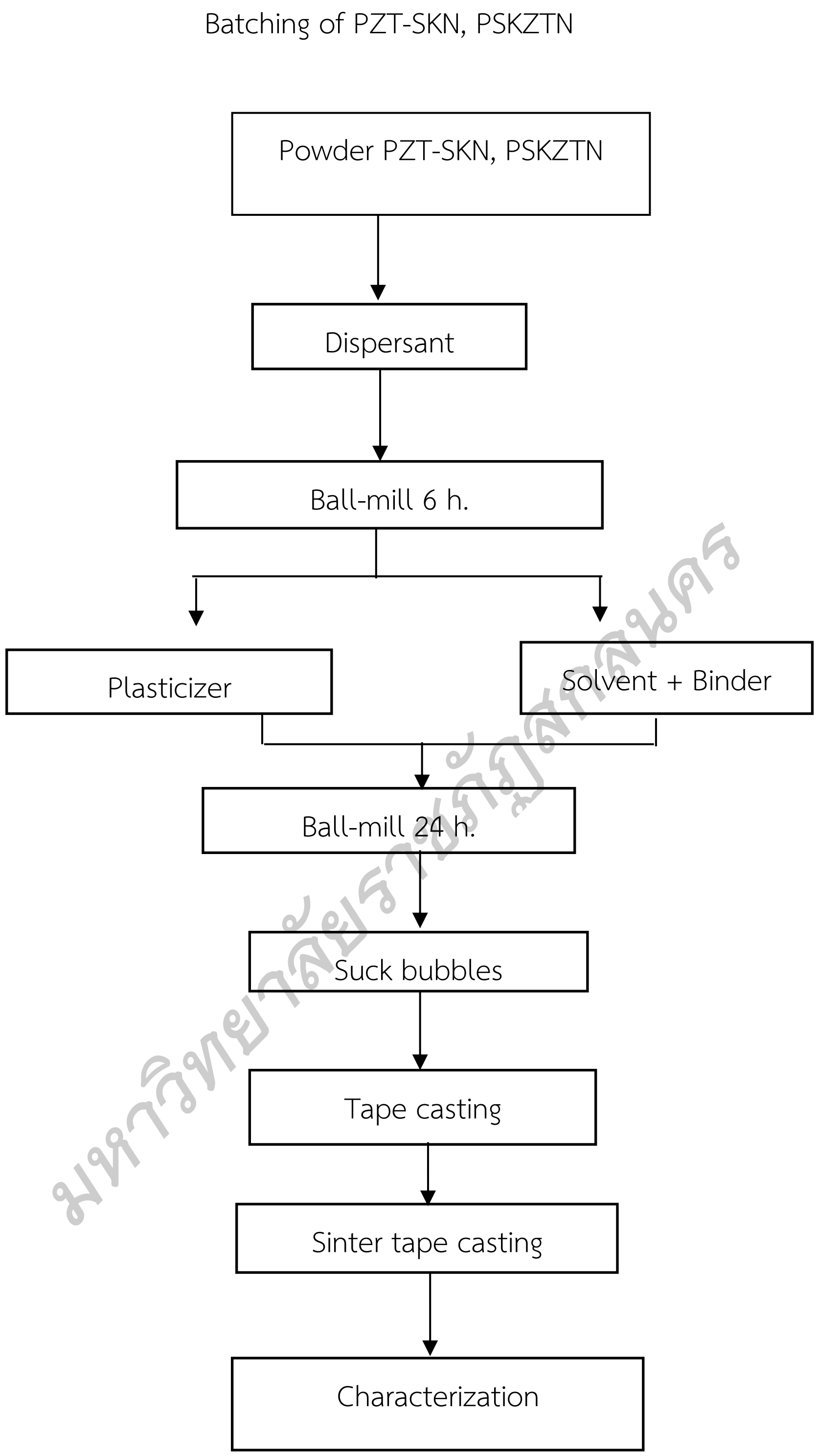
Batching of PZT-SKN, PSKZTN
Powder PZT-SKN, PSKZTN
Dispersant
Ball-mill 6 h.
Plasticizer
Solvent + Binder
Ball-mill 24 h.
Suck bubbles
Tape casting
Sinter tape casting
Characterization

Figure 17 Flow chart for the processing of PZT-SKN and PSKZTN

4. Microstructure of the samples

X-ray diffraction is the elastic scattering of x-ray photons by atoms in a periodic lattice. The scattered monochromatic x-rays that are in phase give constructive interference. Figure 11 illustrates how diffraction of x-rays by crystal planes allows one to derive lattice spacings by using the Bragg' s law.

$$n\lambda = 2d\sin\theta \tag{3.3}$$

where n is an integer called the order of reflection, λ is the wavelength of x-rays, d is the characteristic spacing between the crystal planes of a given specimen and θ is the angle between the incident beam and the normal to the reflecting lattice plane. By measuring the angles, θ, under which the constructively interfering x-rays leave the crystal, the interplanar spacings,

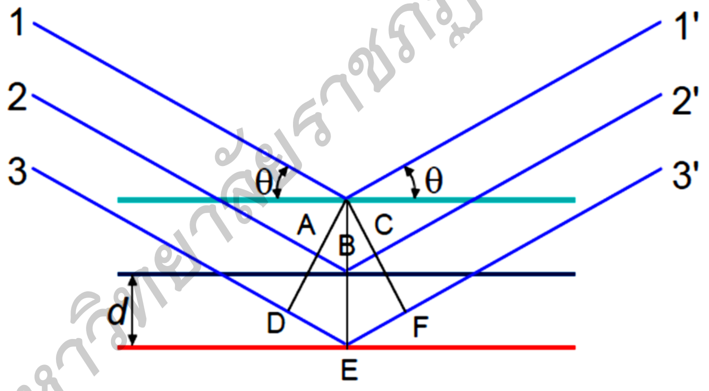

Figure 18 Principle of x-ray diffraction analysis.

Figure 19 Shimadzu X–Ray Diffractmeter 6100

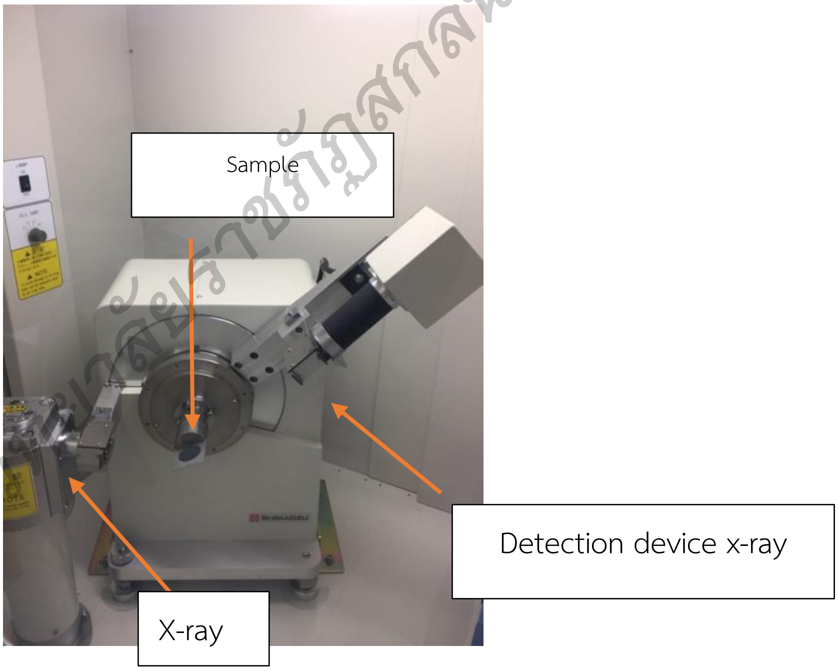
Sample
Detection device x-ray
X-ray

Figure 20 X-ray source sample input characteristics and X-ray inspection equipment.

5. Properties of the samples

5.1 Density

The density measured using the standard Archimedes method. The volumetric density was measured of an object divided by its volume.

$$\rho = \frac{A}{|B|} \times (\rho_0 - d) + d \tag{3.4}$$

Where ρ is density of sample, A is weight air, B is weight in water, ρ_0 is density of water and d is density of air.

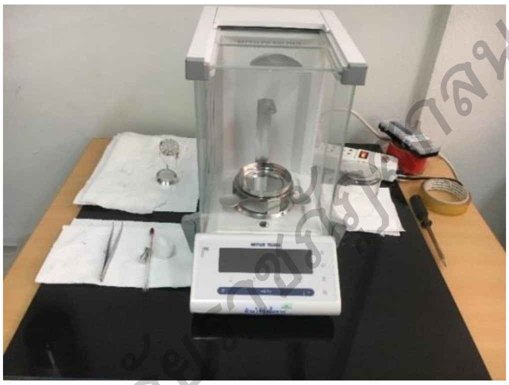

Figure 21 Density Kit on Center of Excellence on Alternative Energy at Sakon Nakhon Rajabhat University.

5.2 Vickers Hardness

The Vickers Hardness was measured by micro hardness tester. The Vickers test is often easiest to use than hardness test cab be required calculation are independent of the size of the indenter can be used for all materials irrespective of hardness. We measured at room temperature by micro hardness test with varies loads of ,0.05 N at 10 seconds, and the repeated 3 times for each sample, and the average hardness measured data. The unit of hardness of our sample given by the is known as the Vickers Pyramid Number (HV) indenter into the surface of the specimen, defined by,

$$HV = \frac{2P_H Sin\theta}{l^2} = 1.8544\frac{P_H}{l^2} \tag{3.5}$$

Where l (mm) is the average diagonal length of the diamond shaped impression made on the indented surface, P_H is the stress of the indenter. The unit of the Vickers hardness can be used GPa, given by 3.5

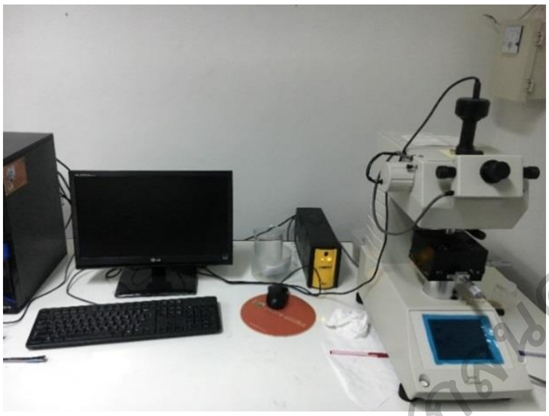

Figure 22 Vickers hardness tester model series.

5.3 Scanning electron microscope (SEM)

The SEM is a microscope which uses electrons to illuminate a sample, instead of visible light used in optical microscope. When an electron beam strikes the sample, a variety of signals are generated. The three signals which mostly perform in SEM are secondary electrons, backscattered electrons and X-rays. Secondary electrons (SE) provide fine structure topographical feature of sample surface, backscattered electrons (BE) are used to discriminate areas of different atomic number elements and X-rays are used to identify the composition and measure the amount of elements in the sample. The SEM operates in high vacuum so the living samples, liquids and anything that contains liquids must be dried before observing. The SEM of model TM4000Plus is equipped with the low vacuum mode and enables to observe non-metal coating sample. The specification of this model is tungsten filament source, 3.0 nm resolution at HV mode and 4.0 nm resolution at LV mode, x5 to x300,000 magnification, SE and BE detector. Additional EDS is equipped for qualitative and quantitative, mapping and line scan elemental analysis. EDS limitations: no detection of elements below B, X-ray detection limit 1,000 -2,000 ppm (0.1 – 0.2 %wt.) depending on the element and samples must be no fluids.

มหาวิทยาลัยราชภัฏมหาสารคาม

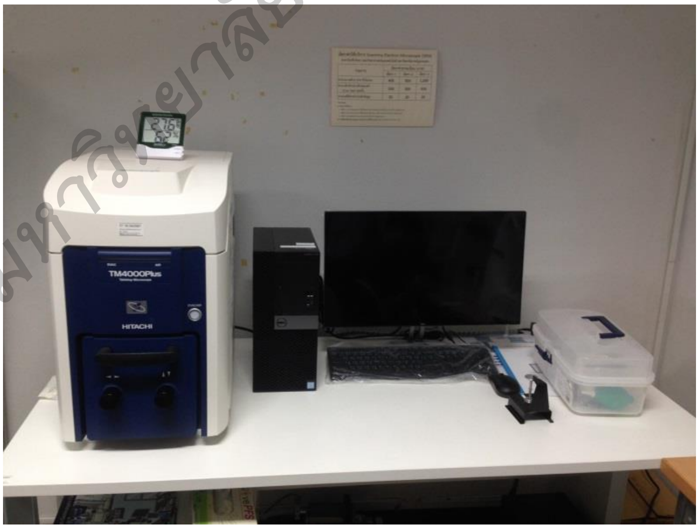

Figure 23 the scanning electron microscope techniques.

6. Ferroelectric Properties Measurement

The samples were coated with silver paint on the sample surfaces as electrode for piezoelectric measurements.

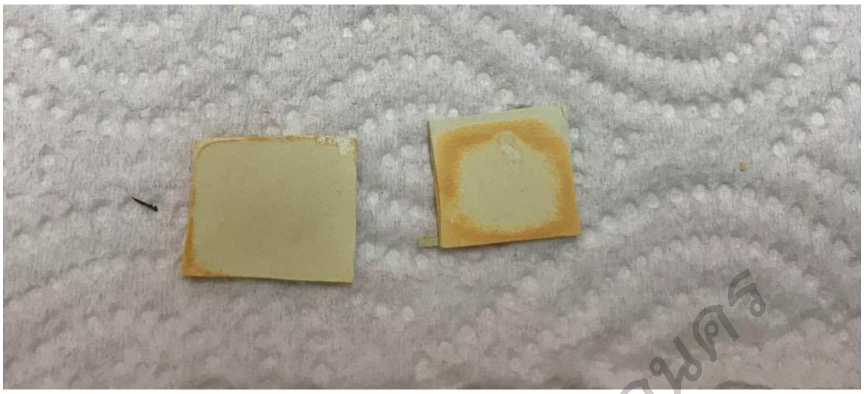

Figure 24 Samples surface was tape ceramic.

6.1 Dielectric properties

In this study, dielectric properties were carried out by capacitances. The capacitances of sample electrode were obtained using Chen Hwa 1061 LCR–Meter connected in a chamber that was heated at a function temperature from 30–600 °C. For the dielectric constants were measured at a discrete frequency range of 1 kHz ,10 kHz and 100 kHz. The capacitances were used to investigate the dielectric constants follow as equation:

$$\varepsilon_r = \frac{ct}{\varepsilon_0 A} \tag{3.4}$$

Where c is the capacitance of the sample, t and A are the thickness and the area of the electric, respectively, and ε_0 is the dielectric permittivity in vacuum (0.08854 pF/m^{-1}).

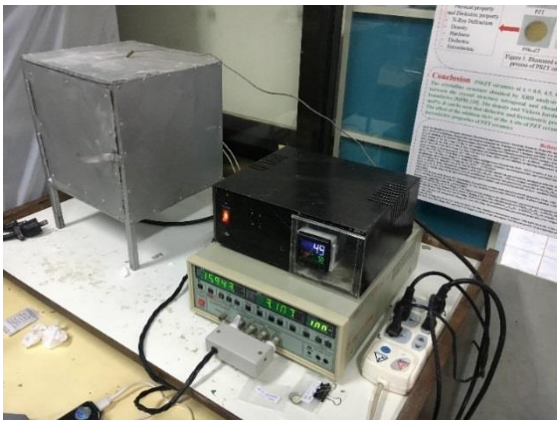

Figure 25 the measurement was carried out by Chen Hwa 1061 LCR–Meter.

6.2 Polarization hysteresis loop

The characteristic of hysteresis loop was observed with polarization-electric field (P-E loop) using high voltage AC amplifier (Trek, model 20/20C-HS), applying low field into the sample, connecting to Sawyer-Tower circuit, and transform signal to Pico scope for interpreted hysteresis loop shown in Figure 26

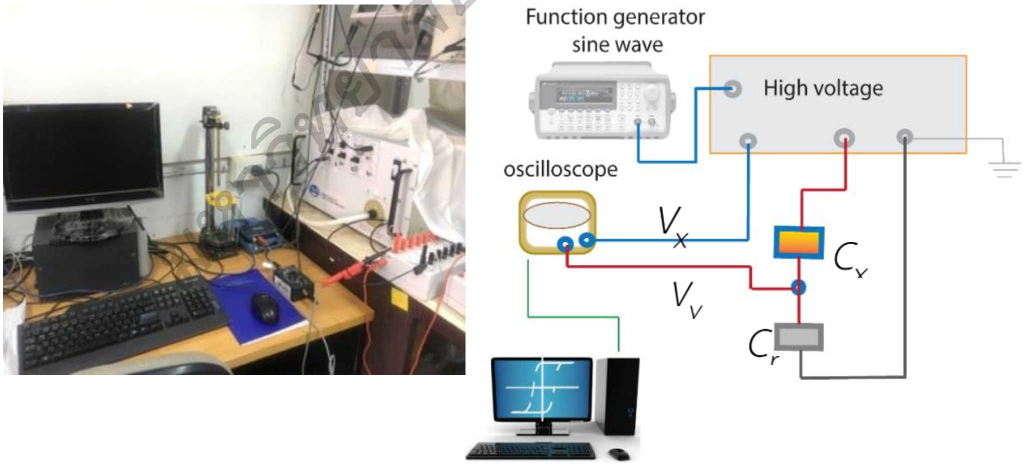
Function generator
sine wave
High voltage
oscilloscope
V_x
V_y
C_x
C_r

Figure 26 the investigate characteristics Sawyer-Tower circuits.
(Sawyer & Tower., (1930)

6.3 Piezoelectric coefficient (d_{33})

Because a piezoelectric ceramic is anisotropic, physical constants relate to both the direction of the applied mechanical or electric force and the directions perpendicular to the applied force. Consequently, each constant generally has two subscripts that indicate the directions of the two related quantities, such as stress (force on the ceramic element / surface area of the element) and strain (change in length of element / original length of element) for elasticity. The direction of positive polarization usually is made to coincide with the Z-axis of a rectangular system of X, Y, and Z axes (Figure 20). Direction X, Y, or Z is represented by the subscript 1, 2, or 3, respectively, and shear about one of these axes is represented by the subscript 4, 5, or 6, respectively. Definitions of the most frequently used constants, and equations for determining and interrelating these constants, are summarized here. The piezoelectric charge constant, d, the piezoelectric voltage constant, g, and the permittivity, e, are temperature dependent factors.

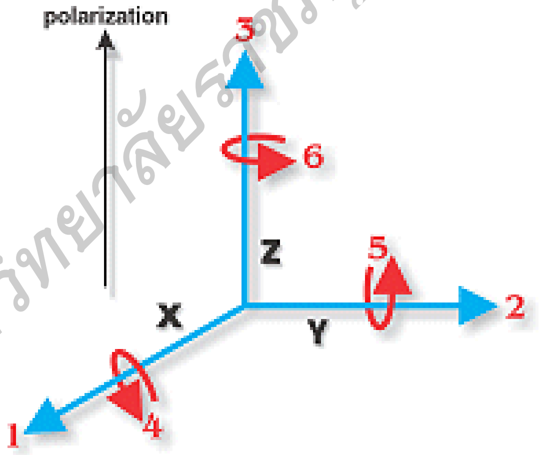

Figure 27 The direction of positive polarization usually is made to coincide with the Z-axis.

The piezoelectric charge constant, d, is the polarization generated per unit of mechanical stress (T) applied to a piezoelectric material or, alternatively, is the mechanical strain (S) experienced by a piezoelectric material per unit of electric field applied. The first subscript to d indicates the direction of polarization generated in the material when the electric field, E, is zero or, alternatively, is the direction of the applied field strength. The second subscript is the direction of the applied stress or the induced strain, respectively. Because the strain induced in a piezoelectric material by an applied electric field is the product of the value for the electric field and the value for d, d is an important indicator of a material's suitability for strain-dependent (actuator) applications. d_{33} induced polarization in direction 3 (parallel to direction in which ceramic element is polarized) per unit stress applied in direction 3 or induced strain. In direction 3 per unit electric field applied in direction 3

Measurement of vibration coefficient (d_{33}). Measurement of vibration coefficient (d_{33}) . Display d_{33} with a d_{33} meter series. The equation for d_{33} is

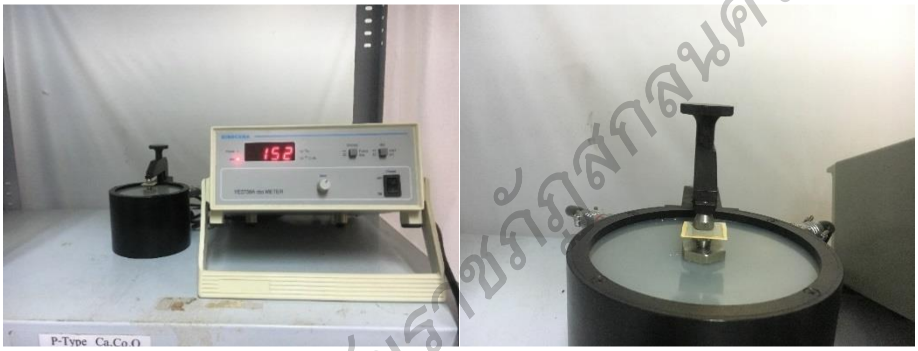

(a) (b)

Figure 28 (a) d_{33} meter (b) testing piezoelectric coefficient of the sample.

7. Piezoelectric module

Piezoelectric modules consists of piezoelectric materials that have been induced by an electrode. After that, take the terminal with copper sheets on both sides is the negative and the positive side and connect the wires on both sides in order to measure the voltage difference from the conversion of mechanical energy to the electric potential is shown in Figure 30.

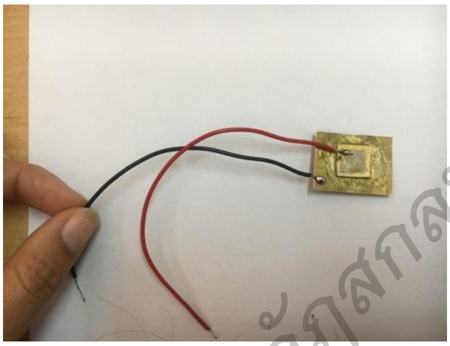

Figure 29 The characteristics of Piezoelectric Modules.

Measuring the electric potential difference from the conversion of mechanical energy to the electric potential of the ceramic tape modulo dielectric This is achieved by placing the piezoelectric modules into a mechanical energy diversion into the electric potential difference for the piezoelectric module. After that, measure the electric potential difference from the oscillation test by using a frequency generator in which the electric potential is a direct electric voltage it involves the energy of piezoelectric materials is shown in Figure 31.

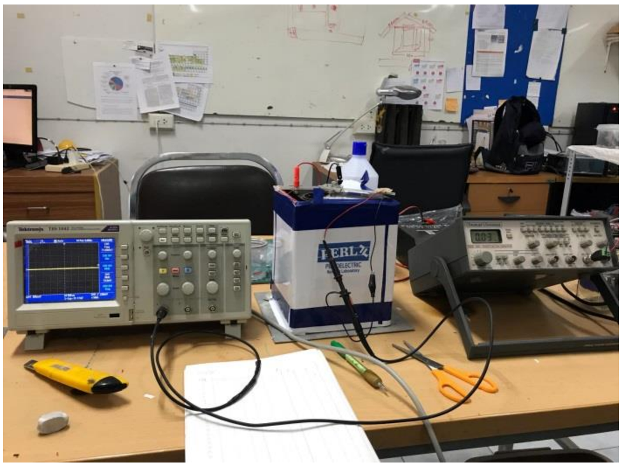

Figure 30 Measuring the electric potential difference from a change in mechanical energy to the electric potential

CHAPTER 4

RESULTS AND DISCUSSION

This chapter presents the synthesized of PZT-SKN and PSKZTN. The results in the PZT-SKN tape ceramic is investigated on the crystalline structure by X-ray diffraction, relative density and Vickers Hardness. Generally, ferroelectric material is determined by dielectric property and polarization electric field loops of PZT-SKN and PSKZTN tape ceramic.

PHASE STRUCTURE

PZT-SKN powder inspection results with X-ray diffraction technique.

In this experiment, PZT-SKN powder was prepared by composite method. The PSKZTN powder was prepared by oxide mixture by calcined at 850°C. The duration of the burn was 4 hours, using the rate of increase and decrease of temperature to 5°C per minute. From the test results of calcined PZT-SKN and PSKZTN materials using X-ray diffraction technique. Is was found that the X-ray diffraction pattern is shown in Figure 31 and 32 respectively.

The phase purity of samples was determined from the calcined powder pellets. X-ray diffraction was carried out in a Shimadzu XRD Diffract meter 6100. Scans of 2θ from 20° to 60° were used to collect data. Figure 30 shows the XRD pattern for PZT-SKN. From the synthesis of PZT-SKN material by composite method the calcine at 850°C temperature began to appear in the PZT-SKN phase but the phase was not complete. In which undesired phase occurs which can be observed from the peak of XRD in different angles at approximately which is a substance in the reaction.

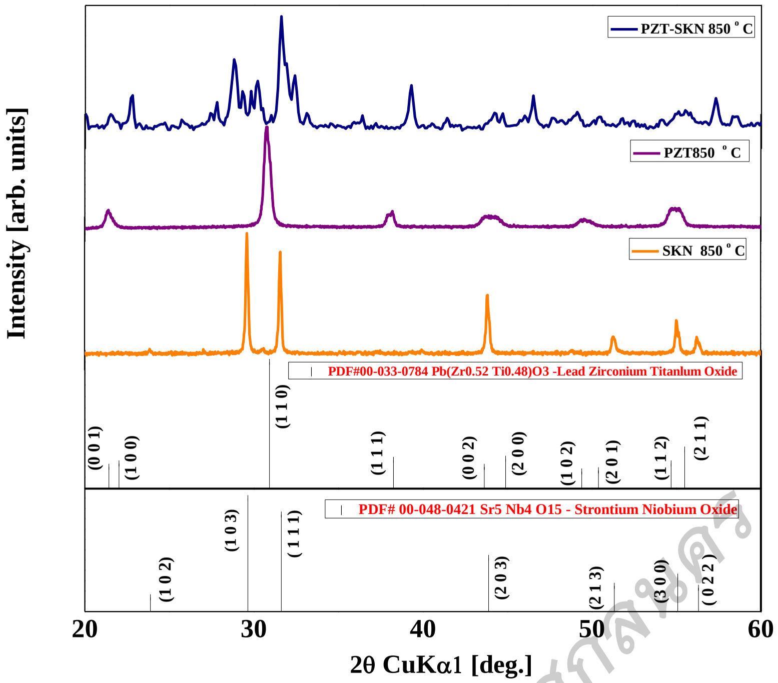

Figure 31 XRD graph of calcine powder 0.975Pb (Zr$_{0.52}$, Ti$_{0.48}$) O$_3$-0.02Sr (K$_{0.25}$, Nb$_{0.75}$) O$_3$; (PZT-SKN) from incineration at impurities at 850 ° C.

PSKZTN powder inspection results with X-ray diffraction technique.

The synthesis of piezoelectric PSKZTN materials by the mixed oxide method the sintering 850 ° C began to appear in the phase of PSKZTN. Shows the XRD pattern for PSKZTN matching the pattern for Pb(Zr$_{0.58}$Ti$_{0.42}$)O$_3$. The 001 and 002 peaks, located at 2θ values of 21-23° and 43-44° respectively, indicate whether PZT is in the rhombohedral or tetragonal phase. If the material is tetragonal. The different lattice parameters for a and b will cause different reflections, causing the (001) and (100) peaks. In rhombohedral sample, a=c, so the peaks do not split.

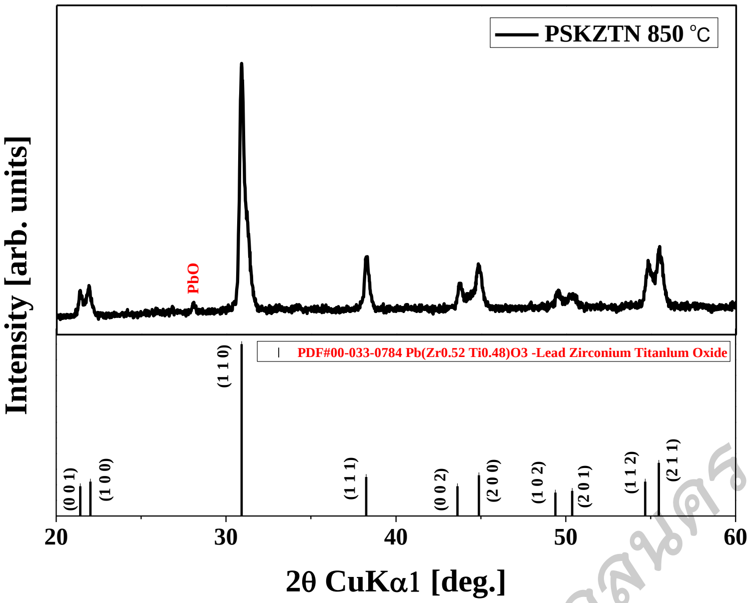

Figure 32 XRD patterns of ceramic powder $Pb_{0.97}Sr_{0.02}K_{0.05}$ [$(Zr_{0.58}$ $Ti_{0.42})$ 0.985$Nb_{0.015}$]O_3; (PZTSKN) from incineration at impurities at 850 °C.

The result of inspection of the binder of the ceramic tape with X-ray diffraction technique (XRD)

The binder of the tape ceramic at a temperature of 750 °C for 1, 2 and 3 h. X-ray diffraction was carried out in a Shimadzu X–Ray Diffract meter 6100. Scans of 2θ from 20° to 60° were used to collect data. It was found that the structure is no different when crystallized, it was found that burning of the binder at 2 h. was a suitable time for the tribe to banish the binder in order to be further burned. Show as Figure 33.

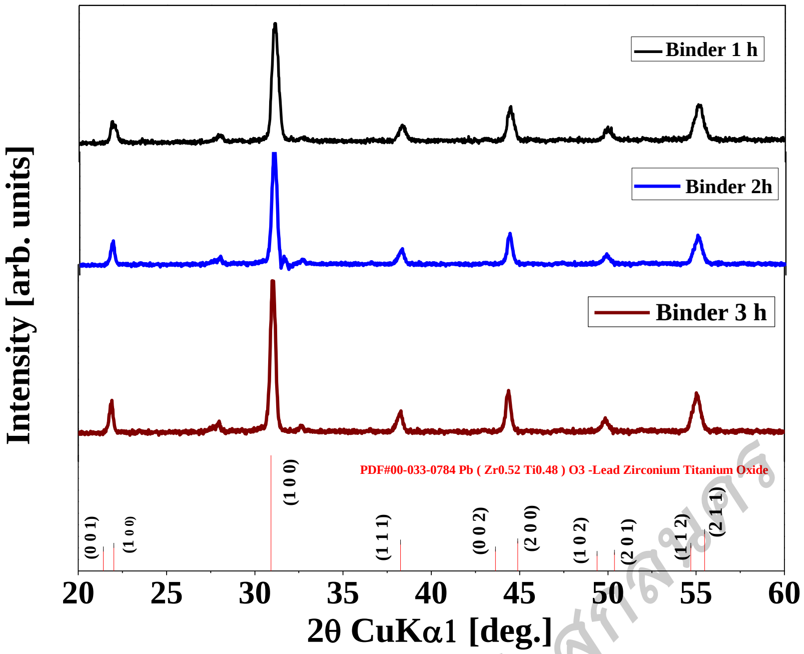

Figure 33 The XRD patterns of PSKZTN ceramic tapes, burned for binding 1, 2 and 3 hours, temperature 750 °C.

The results of the examination of ceramic tape of PZT-SKN and PSKZTN with X-ray diffraction technique.

The results of PZT-SKN ceramic tape inspection by X-ray diffraction technique.

In addition, the ceramic tape was sintered at 1100 °C for 2 hours. The ceramic tape the measurements consist of 1 layer, 3 layers and 5 layers. From the sintering of sintered tapes using X-ray diffraction (XRD) techniques, the X-ray diffraction pattern is shown. In Figure 34. It was found that PZT-SKN of the microstructure examination of the X - ray diffraction (XRD) technique, it was found that the PZT-SKN exhibited a tetragonal structure more than the perovskite structure. However, the density and hardness of the Vickers Hardness shows that the physical properties are not much different.

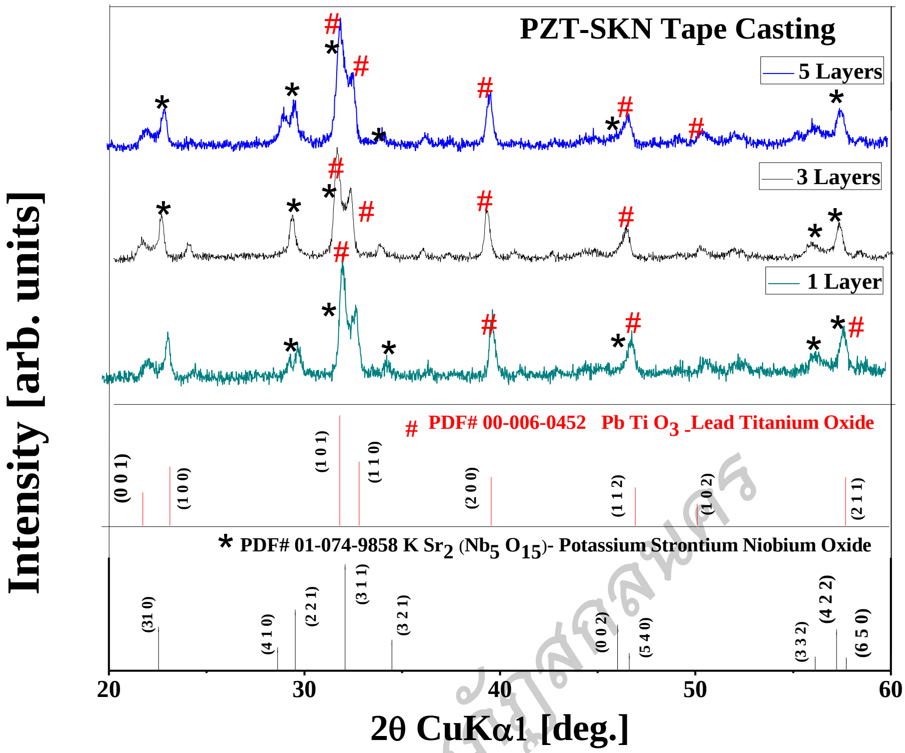

Figure 34 The XRD graph of the PZT-SKN ceramic tape, 1 layer, 3 layers and 5 sintered layers at 1100 ° C.

The results of PZT-SKN ceramic tape inspection with X-ray diffraction techniques.

In addition, tape ceramic at 1100 °C. The result of the analysis from the measurement graph using X-ray diffraction technique. of 1 layer, 3 layers and 5 layers of tape ceramic in the conditions of sintering, binder at 2 h. It was found that PSKZTN has a foreign peak and also shows that a composite structure between the tetragonal and rhombohedral of morphotropic phase boundary (MPB). Show as Figure 35.

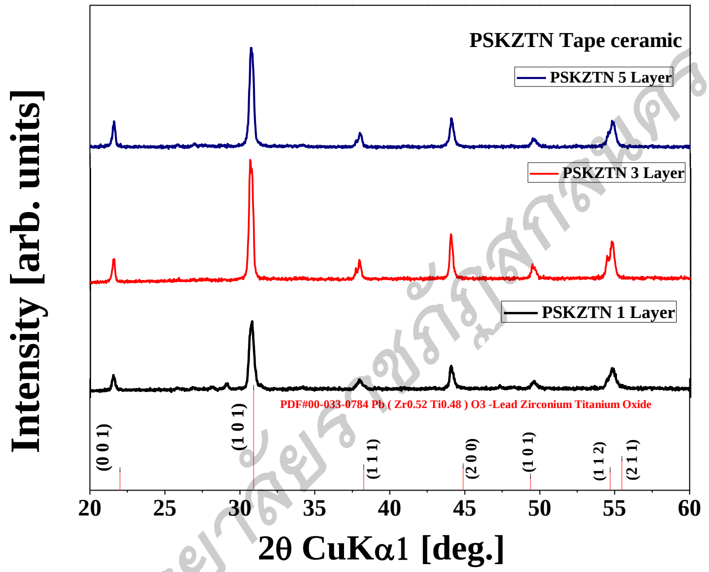

Figure 35 The XRD patterns of PSKZTN ceramic tape, 1 layer, 3 layers and 5 Layers at 1100 °C.

PHYSICAL PROPERTIES

Physical properties PZT-SKN and PSKZTN of tape ceramics.

Table 4 show the results of calculation data base from XRD patterns to lattice parameter, experimental density and relative density. It was found that the density of the example was measured by the Archimedes method using distilled water and in air (Huan et al., 2014). The bulk density of sample increase with increasing composite content. For the fillers, both the PZT-SKN and PSKZTN can be enhancing density increased, according on tend have the density with.

Tape ceramic were sintering at 1100 °C for 2 h. It was found that the physical characteristics of the tape ceramic are light yellow in color. The surface of the tape ceramic on both sides is smooth without cracks or pores. And does not cause bending at the edges, sufficiently firm, not brittle or broken. When comparing the density and weight of the tape ceramic, measured before and after burning, sintering found that the prepared tape had shrinkage throughout the workpiece. This contraction will vary with the sintering temperature, including the sintering time. sintering with details in the Table 4.

Table 5 XRD data of the PZT-SKN and PSKZTN evaluated to the lattice parameters ***a*, *c*** and tetragonal ***c/a***, density (g cm^{-3}), Theoretical Density (g cm^{-3}) relative density (%) and Vickers Hardness (N mm^{-2}).

Powder	*a* (Å)	*c* (Å)	c/a	Density (g cm^{-3})	Theoretical Density (g cm^{-3})	Relative Density (%)	Vickers Hardness (N mm^{-2})
PZT-SKN 1 Layer	0.38637	0.40831	1.056	5.245	7.22	72.27	107
PZT-SKN 3 Layer	0.3920	0.4083	1.041	5.421	7.01	77.3	111
PZT-SKN 5 Layer	0.3902	0.4086	1.047	5.674	7.07	80.2	120
PSKZTN 1 Layer	0.40195	0.4140	1.030	5.696	6.58	86.6	125
PSKZTN 3 Layer	0.40168	0.4128	1.027	5.765	6.61	87.3	129
PSKZTN 5 Layer	0.4006	0.4125	1.029	5.887	6.65	88.6	153

MICROSTURCTURE

The SEM micrographs of PZT-SKN and PSKZTN tape ceramics 1 layer, 3 layers and 5 layers were sintering at 1100 °C for 2 h. It was found that the distribution characteristics, tight arrangement and the grain size is different as follows.

The results of the examination of the microstructure of tape ceramic PZT-SKN.

The SEM micrographs of PZT-SKN tape ceramic 1 layer, 3 layers and 5 layers were sintering at 1100 °C for 2 h. It was found that the grains of ceramics had many sizes of grains, which spread in some areas where the edges of the grains were partially connected. Therefore, causing bad adhesion in addition, it was found that the grains were unevenly arranged in size. Therefore, creating a large gap spread throughout the substance. The details are as follows.

Figure 36 shows the SEM morphology of the PZT-SKN tape ceramic 1 layer were sintering at 1100 °C for 2 h. It was mentioned in our previous reported that the grain growth in fabrication route of PZT-SKN ceramics give promoted by doping with a single acceptor or single donor samples, which had the lowest grain sizes. There is some argument that adding both an acceptor and a donor will effectively cancel each other out in grain size effects. (Joseph Robert et al., 1999). With PZT-SKN tape ceramic 1 layer exhibited clear grain boundary and porosity, indicating that it was not fully densified as shown in Figure 37. The grain of tape ceramic a cubic ceramic with grains of various sizes spread everywhere In which the edges of the grain are partially melted together resulting in poor coagulation of grain in addition, it was found that the grains were unevenly arranged, resulting in large gaps scattered throughout the substance.

Figures 36-38 show the SEM morphology of the PZT-SKN tape ceramic 3 and 5 layers were sintering at 1100 °C for 2 h. It was found that grain has many shapes mixed together. By not being able to clearly distinguish the boundaries of grain because there is melting and sticking together throughout the tape ceramic. After the inspection of PZT-SKN 1, 3, and 5 layers of ceramic tape using the SEM technique with an extension of 3.00 μm, the average grain size of the ceramic tape can be determined by the linear count method. intercept) the average grain size further increased from 2.5 ± 0.4 μm, 2.5 ± 0.2 μm and 2.3 ± 0.2 μm.

The SEM morphology of the PZT-SKN tape ceramic measured density data found that there is a coherent grain by tape ceramic at 5 layers with the thickness of the tape ceramic at 0.8 mm resulting in tape ceramic higher density values.

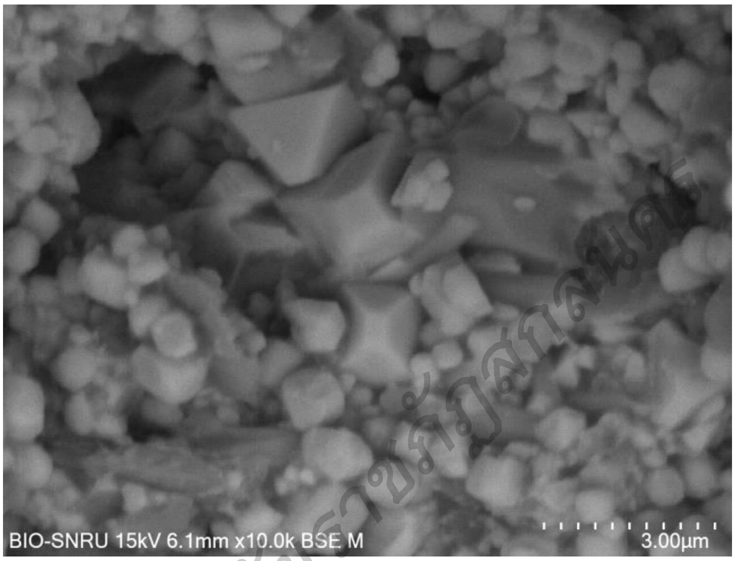
BIO-SNRU 15kV 6.1mm x10.0k BSE M
3.00μm

Figure 36 SEM image of PZT-SKN tape ceramic 1 layer.

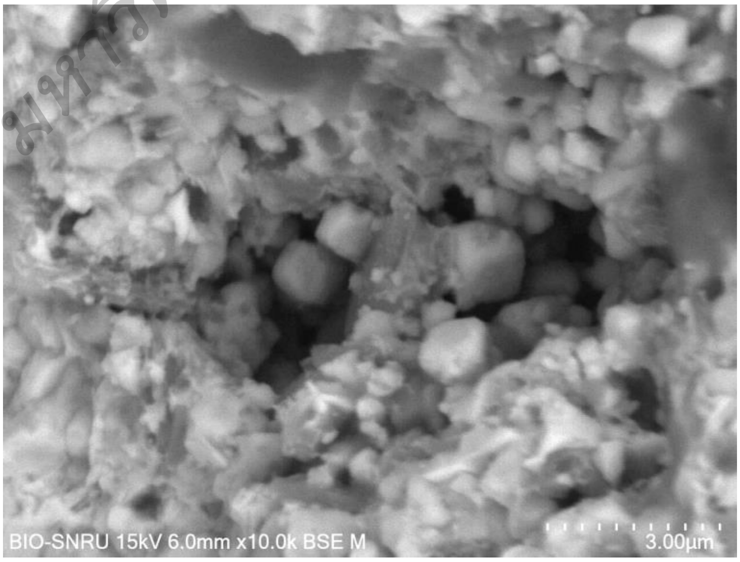
BIO-SNRU 15kV 6.0mm x10.0k BSE M
3.00μm

Figure 37 SEM image of PZT-SKN tape ceramic 3 layers.

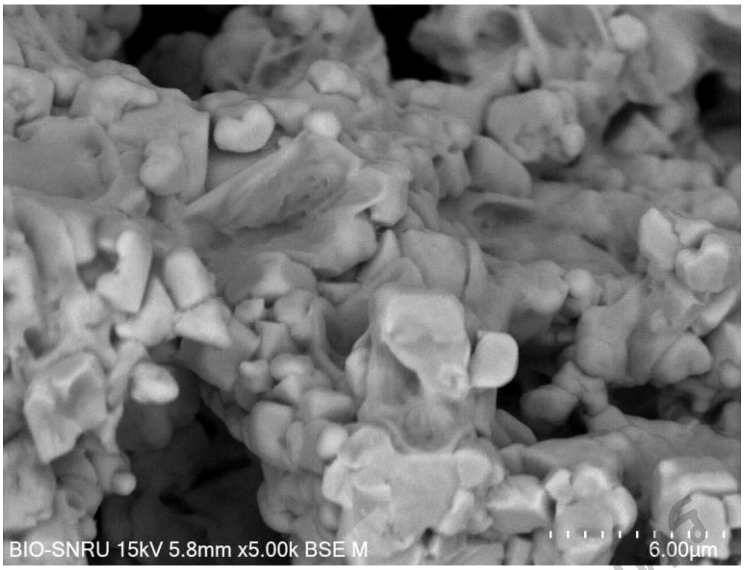

Figure 38 SEM image of PZT-SKN tape ceramic 5 layers.

The results of the examination of the microstructure of tape ceramic PSKZTN.

The SEM micrographs of PSKZTN tape ceramics 1 layer, 3 layers and 5 layers were sintering at 1100 °C for 2 h as display in Figures 39-41. It was found that the grain of the ceramic has a square shape but has melted together throughout the work piece resulting in very tight adhesion and has a high-volume shrinkage. It was mentioned in our previous reported that the grain size increase with longer sintering hold times, and slightly decreased on annealing in nitrogen. Normally, doping with a single acceptor or a single donor with act to decrease grain size. (By Joseph Robert Scholz.,2009). With PSKZTN tape ceramic exhibited clear grain boundary and porosity, indicating that it was not fully densified as shown in Figure 39. tape ceramic at PSKZTN 1 layer there is still a remaining binder. Normally, it should increase the density of the tape. But because the sintering temperature is high enough to lead the evaporation of large amounts of lead Therefore creating a larger gap as can be seen from the large pores scattered in the structure. After the inspection of PSKZTN 1, 3, and 5 layers of ceramic tape using the SEM technique with an extension of 3.00 $\mu\mathrm{m}$, the average grain size of the ceramic tape can be determined by the linear count method. intercept) the average grain size further increased from 2.8 ± 0.4 $\mu\mathrm{m}$, 2.5 ± 0.2 $\mu\mathrm{m}$ and 2.7 ± 0.5 $\mu\mathrm{m}$.

The SEM morphology of the PSKZTN tape ceramic is a corresponding grain by being melted together in cubes throughout the tape ceramic resulting in very tight adhesion and high-volume shrinkage. Normally it should increase the density of the plates tape ceramic but because the temperature in the sintering of crystals is high enough to cause the lead to evaporate in high amounts, causing a larger gap. As can be seen from the pores that spread in the structure

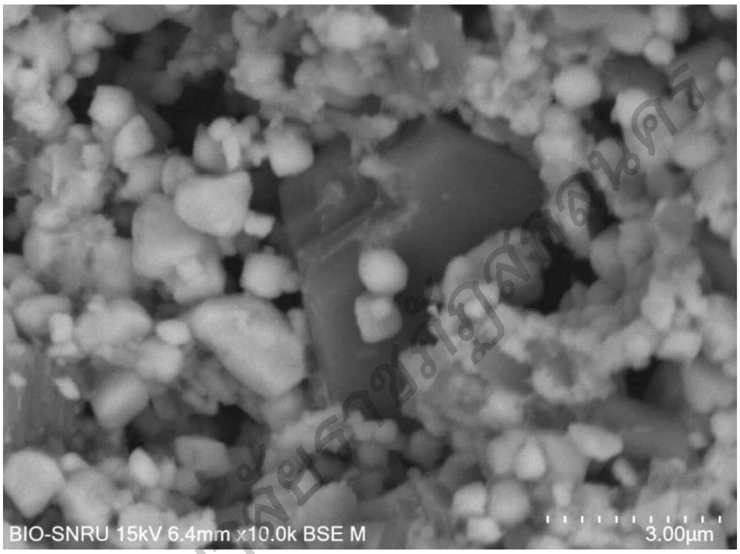
BIO-SNRU 15kV 6.4mm x10.0k BSE M
3.00µm

Figure 39 SEM image of PSKZTN tape ceramic 1 layer.

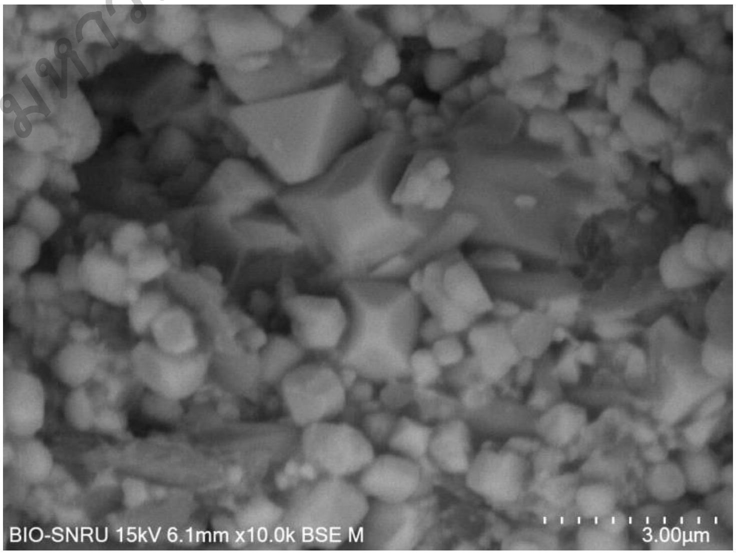
BIO-SNRU 15kV 6.1mm x10.0k BSE M
3.00µm

Figure 40 SEM image of PSKZTN tape ceramic 3 layers.

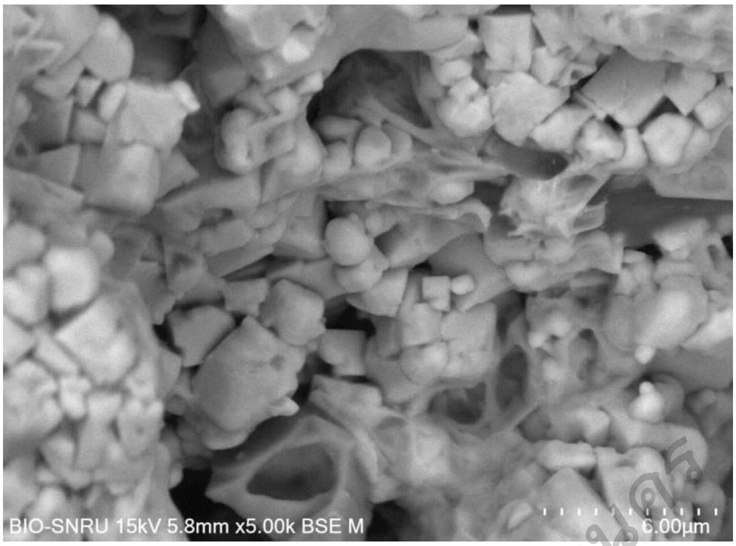
BIO-SNRU 15kV 5.8mm x5.00k BSE M
6.00µm

Figure 41 SEM image of PSKZTN tape ceramic 5 layers.

DIELECTRIC PROPERTIES

Tape ceramic PZT-SKN and PSKZTN through polarization and will be used to measure the electrical capacity (c) and dielectric loss ($\tan\delta$). That changes with the temperature of the LCR-Meter. The electrical capacitance values will be used in the calculation dielectric constant (ε_r) of tape ceramic as equation 3.4 shown in Chapter 3.

Dielectric properties PZT-SKN

The PZT-SKN at 1 layer, 3 layers and 5 layers tape ceramics. Measure the electrical capacity and the value dielectric loss ($\tan\delta$) of frequency 1 kHz, 10 kHz and 100 kHz that is measured during the temperature range of 32 – 600 °C, the experimental results are as follows.

In addition, based on the temperature characteristics of Figure 42-44 shows the PZT-SKN at 1 layer, 3 layers and 5 layers tape ceramic. The graphs show dielectric constant (ε_r) and dielectric loss ($\tan\delta$).The calculations have increased steadily and when measured to 600°C, dielectric constant (ε_r) also increased. Therefore, cannot determine the Curie temperature of the tape ceramic due to limitations in the instrument likewise. The graph shows the relationship between. dielectric loss ($\tan\delta$) versus temperature the graph dielectric loss ($\tan\delta$) steadily increasing.

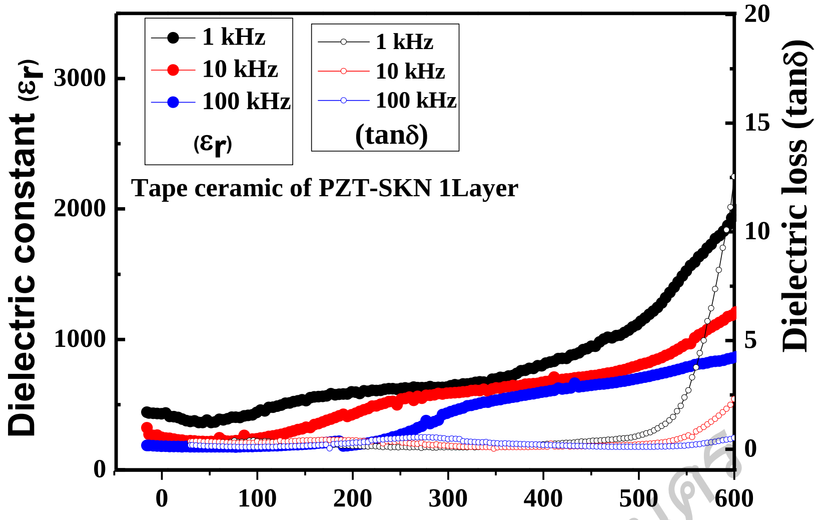

Figure 42 The dielectric constant and dielectric loss dependent on temperature of PZT-SKN tape ceramic 1 layer.

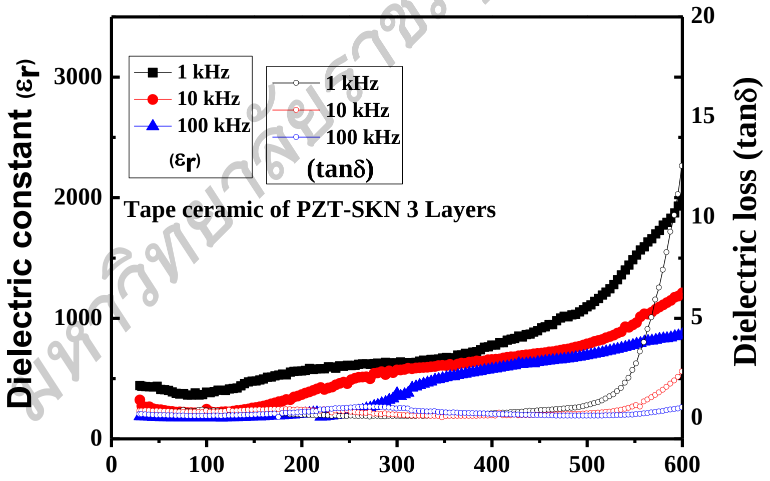

Figure 43 The dielectric constant and dielectric loss dependent on temperature of PZT-SKN tape ceramic 3 layers.

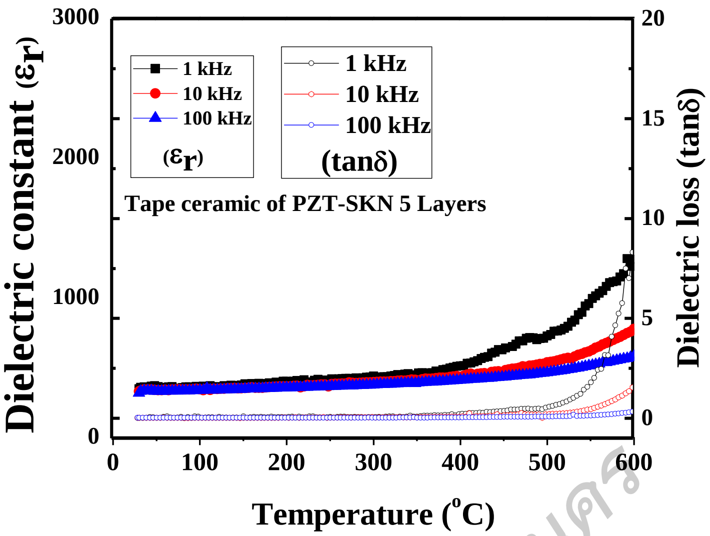

Figure 44 The dielectric constant and dielectric loss dependent on temperature of PZT-SKN tape ceramic 5 layers.

Dielectric properties PSKZTN

The PSKZTN at 1 layer, 3 layers and 5 layers tape ceramics exhibits the temperature dependent dielectric properties of the sintered ceramics measure at difference frequency as display in Figure 45-47.

In addition, based on the temperature characteristic of PZT-SKN at 1 layer, 3 layers and 5 layers. The graphs show features to the highest dielectric constant (ε_r) at 9,524, 18,006 and 41,224 (at 1 kHz) and dielectric maximum temperature ($T_{\max}$) at 530, 532 and 526 °C for PZT-SKN. respectively at 1 kHz frequencies as same dielectric loss ($\tan\delta$) in heat. It was found that at 34, 34 and 37 °C at 1 kHz frequency, dielectric loss was 0.227, 0.208 and 0.755 respectively, resulting in high dielectric properties of PZT.

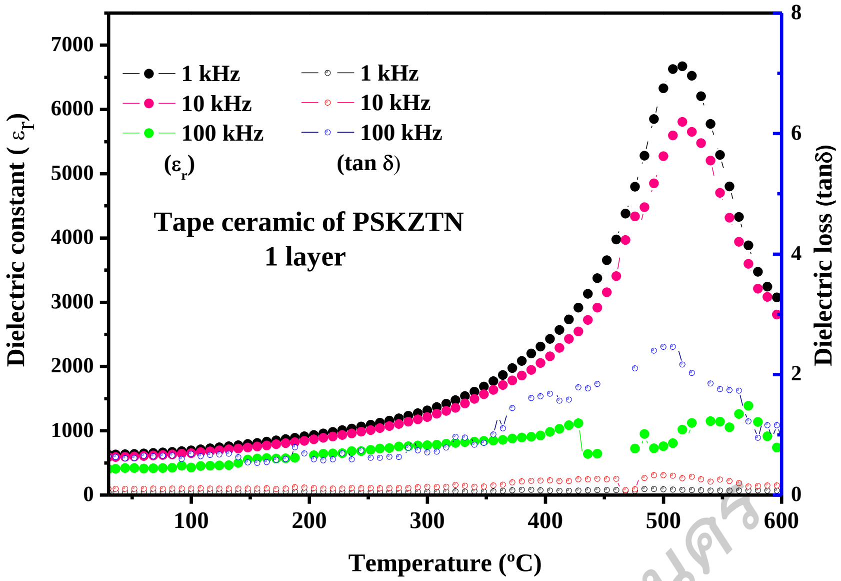

Figure 45 The dielectric constant and dielectric loss dependent on temperature of PSKZTN tape ceramic 1.

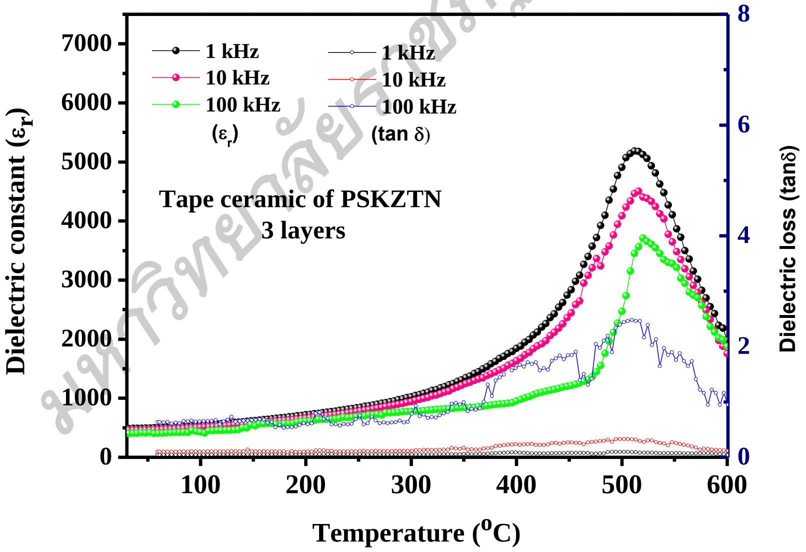

Figure 46 The dielectric constant and dielectric loss dependent on temperature of PSKZTN tape ceramic 3 layers.

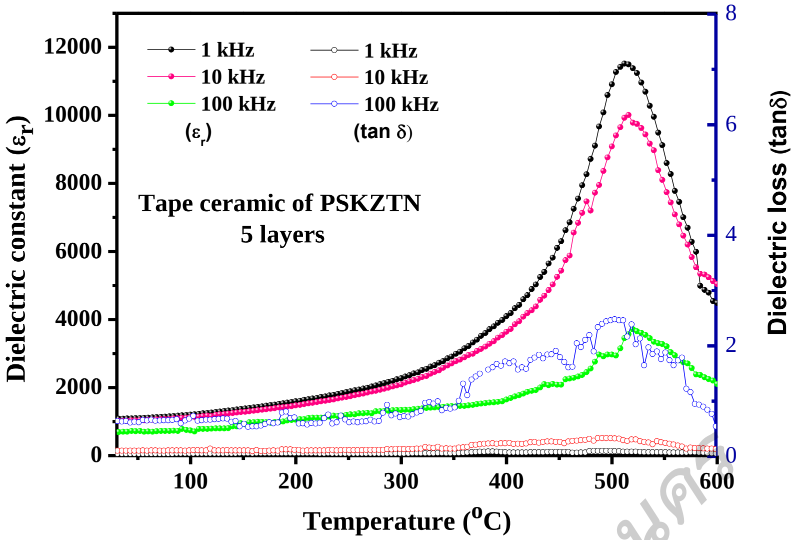

Figure 47 The dielectric constant and dielectric loss dependent on temperature of PSKZTN tape ceramic 5 layers.

FERROELCTRIC PROPERTIES

Ferroelectric properties of PZT-SKN tape ceramic

The measurement of the polarization-electric field (P–E) hysteresis loops was performed to examine the ferroelectric properties of PZT-SKN at 1 layer, 3 layers and 5 layers tape ceramics.

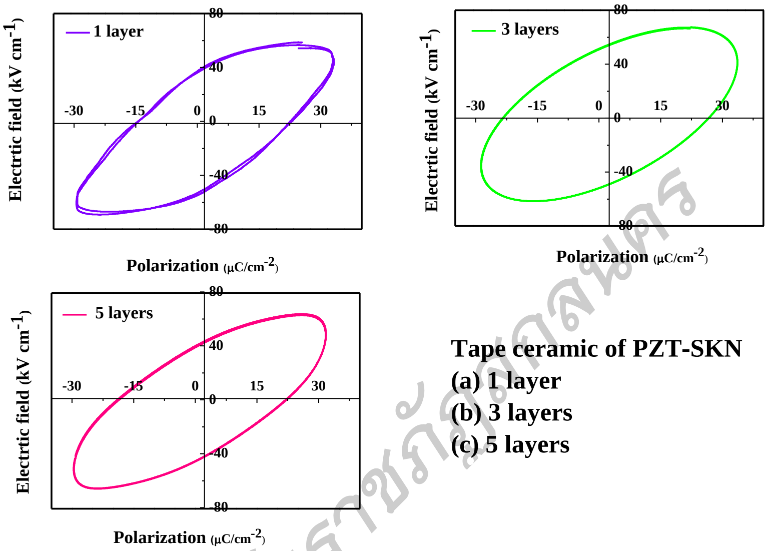

Figure 48 (P-E) Hysteresis loops for PZT-SKN (a)1 layer, (b)3 layers and (c)5 layers ferroelectric tape ceramic.

P-E loop of 1, 2, and 3 layers of PSKZTN ceramics when sintered at 1100 °C at a thickness of 0.50 mm, 0.87 mm and 0.96 that provides a 3 kV mm^{-1} compulsory electric field. For PSKZTN, there is a pressure resistant condition. High voltage found at 1 kV mm^{-1} compulsory electric field shows that when a forced electric field is added will cause the saturated polarizer value of ceramics to increase as shown in the picture and shown in the Table 5.

Table 6 Showing the result of residual polarization (Pr), saturated polarization (Ps), the applicable electric field (E_C) and the piezoelectric coefficient (d_{33}) of the PZT-SKN tape ceramic.

Powder	Pr ($\mu C/cm^2$)	Ps ($\mu C/cm^2$)	Ec (kV cm^{-1})	d_{33} (pC/N^{-1})
PZT-SKN 1 Layer	40.59	25.18	25.15	102
PZT-SKN 3 Layer	45.19	35.47	29.58	112
PZT-SKN 5 Layer	40.00	30.04	25.76	132

Ferroelectric properties of PSKZTN tape ceramic

The measurement of the polarization-electric field (P–E) hysteresis loops was performed to examine the ferroelectric properties of PSKZTN at 1 layer, 3 layers and 5 layers tape ceramics.

From the polarization loop compared with the electric field of PSKZTN, the characteristics of rigid piezoelectric since the squareness loop shows that it uses a lot of energy (Hussain, Sinha, Bhandari, Yadav, & Kumar, 2016).

After the sintering, the tape will be approximately 0.4-0.5 mm thick. The tape will be silver paste to be the electrode of both top and bottom tapes. Then examining the polarization loop relative to the polarize-electric field loop; P-E loop to check polarization.

P-E loop of 1, 2, and 3 layers of PSKZTN ceramics when sintered at 1100 °C at a thickness of 0.47 mm, 0.89 mm and 0.95 that provides a 3 kV mm^{-1} compulsory electric field. For PSKZTN, there is a pressure resistant condition. High voltage found at 1 kV mm^{-1} compulsory electric field shows that when a forced electric field is added Will cause the saturated polarizer value of ceramics to increase as shown in the picture and shown in the Table 6.

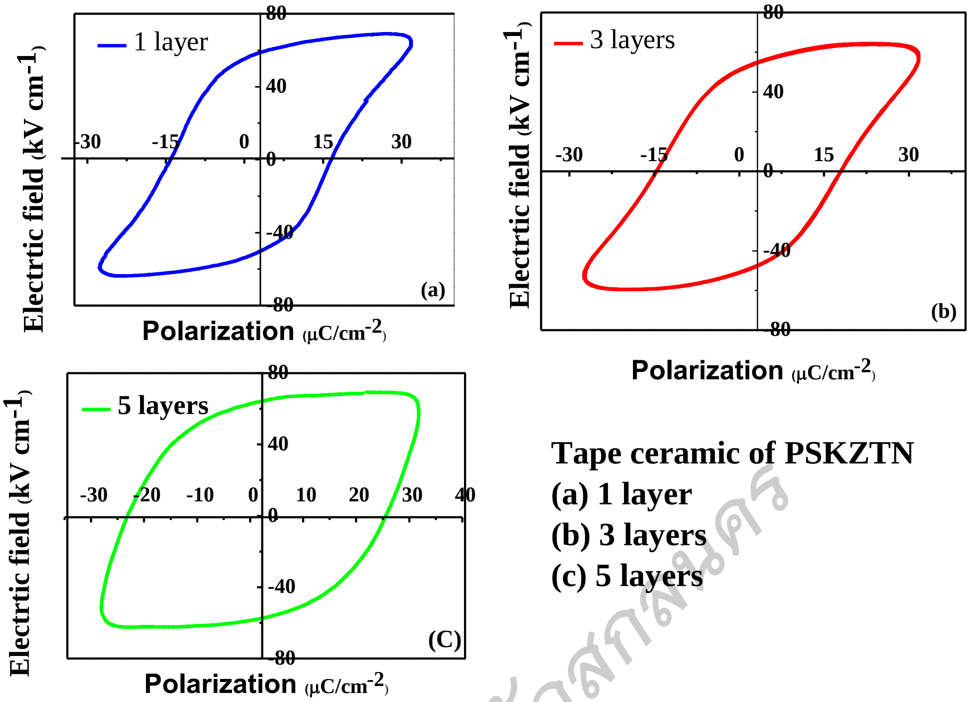

Figure 49 show characteristic the polarization-electric field (P-E) hysteresis loops measurement at room temperature of tape ceramic PSKZTN (a) 1 layer, (b)3 layers and (c) 5 layers.

Table 7 Showing the result of residual polarization (Pr), saturated polarization (Ps), the applicable electric field (E_C) and the piezoelectric coefficient (d_{33}) of the PSKZTN tape ceramic.

Powder	Pr ($\mu C/cm^2$)	Ps ($\mu C/cm^2$)	Ec (kV cm^{-1})	d_{33} (pC/N^{-1})
PSKZTN 1 Layer	58.36	66.21	15.37	115
PSKZTN 3 Layer	40.39	43.78	17.89	156
PSKZTN 5 Layer	64.67	30.54	24.87	174

PIEZOELECTRIC MODULE

The result of measuring the electric potential difference from the conversion of mechanical energy to electrical energy of the piezoelectric modules.

After the invention of the modulo piezoelectric module, the oscillations were used to test the oscillations at different frequencies. In this work, the frequency was tested from 1-20 Hz. PZT-SKN, PSKZTN ceramic tape modules, consisting of 1 layer, 3 layers, and 5 layers by using a mechanical energy diversifier into electrical energy as a source of kinetic energy to the module. Connect the electric circuit directly between the module and the oscilloscope and measure the electric potential difference.

The result of measuring the electric potential difference from the conversion of mechanical energy to electrical energy of PZT-SKN

The divergence of the electrical energy of the PZT-SKN ceramic tape modulo dielectric of 1 layer, 3 layers and 5 layers by using the mechanical energy diversion machine as electrical energy as the source of kinetic energy to the module. direct electrical connection between the module and the oscilloscope measure the electric potential difference as shown in figure 43, it is found that 1 layer of PZT-SKN ceramic tapes at 8 Hz frequency can convert mechanical energy into electrical energy up to 1000 mV. 3 layer PZT-SKN at 9 Hz can change mechanical energy to The maximum electrical power of 1020 mV and 5 layers of PZT-SKN ceramic tapes at 10 Hz can convert mechanical energy into electrical energy up to 980 mV

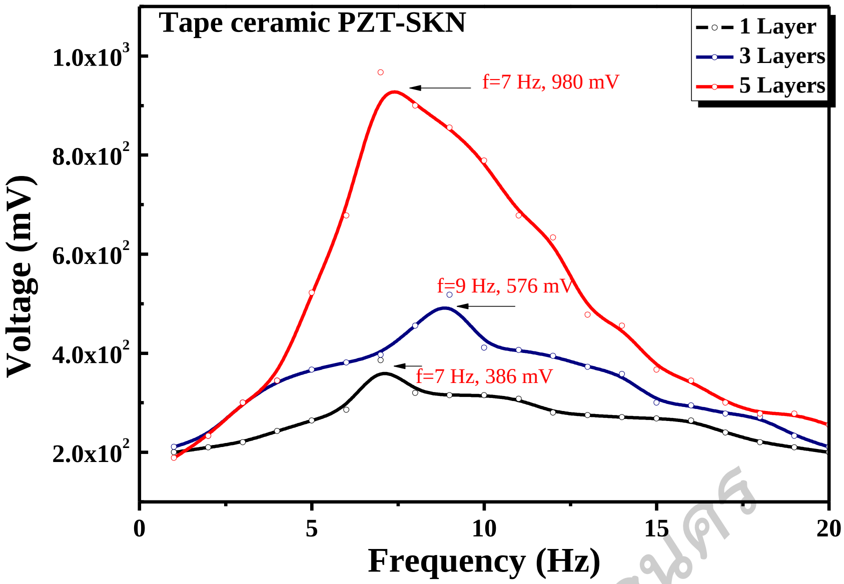

Figure 50 The result of measuring the electric potential difference from the conversion of mechanical energy to electrical energy of tape ceramic PZT-SKN 1 layer, 3 layers and 5 layers.

The result of measuring the electric potential difference from the conversion of mechanical energy to electrical energy of PSKZTN

The divergence of electrical energy of PSKZTN ceramic tape modulo dielectric modules of 1 layer, 3 layers and 5 layers by using the mechanical energy diversion machine as electrical energy as the source of kinetic energy to the module. direct electrical connection between the module and the oscilloscope measure the electric potential difference as shown in Figure 44, it is found that 1 layer of PSKZTN ceramic tape at 10 Hz can convert mechanical energy to maximum electrical power of 1040 mV, while 3 layer PSKZTN at 9 Hz can change mechanical energy to electric power up to 1080. mV and 5 layers of PSKZTN ceramic tape at 9 Hz can convert mechanical energy into electrical energy up to 1060 mV.

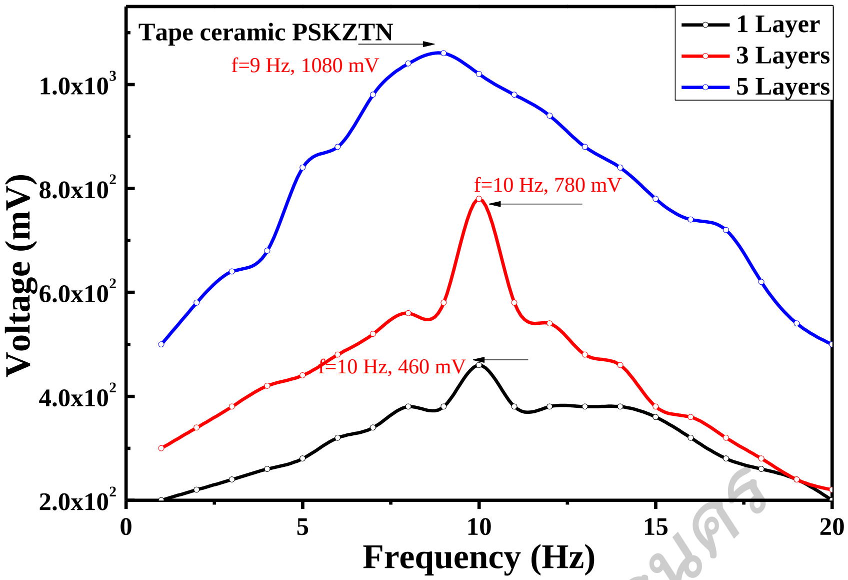

Figure 51 The result of measuring the electric potential difference from the conversion of mechanical energy to electrical energy of tape ceramic PSKZTN 1 layer, 3 layers and 5 layers.

มหาวิทยาลัยราชภัฏพิบูลสงคราม

CHAPTER 5

CONLUSION

This chapter presents the conclusions of the sis title: Fabrication and characterization of piezoelectric tape ceramic for electrical generator. The thesis objectives and suggestion followed the conclusions.

FABRIATE PIEZOELECTRIC CERAMIC TAPE WITH TAPE CASTING

Tape fabrication of piezoelectric tape ceramic materials by fabrication doctor blade process. Sintering, bonding and sintering resulting in a 300-500 μm thickness ceramic tape. When testing the microstructure using XRD technique, it was found that the addition of Sr^{2+} and K^{+} atoms in position A of the Perovskite structure $(A_1A_2)(B'B'')O_3$. Complex type of PZT-SKN and PSKZTN type materials showing the perovskite structure. the tetragonal and rhombohedral of morphotropic phase boundary (MPB).

INVESTINGATE THE DIELECTRIC PROPERTIES POLARIZATION OR THE HYSTERESIS LOOP AND THE PIEZOELECTRIC OF THE PREPARED CERAMIC TAPE

1) Dielectric properties

Dielectric properties test summary ferroelectric properties by studying the behaviors of dielectric constant at different frequencies and temperatures, found that PZT-SKN and PSKZTN exhibits piezoelectric properties because they do not Spread frequency and the result of replacing atoms in position A, showing good ferroelectric properties.

2) Polarization or the hysteresis loop

Summary of polar polarization examination results from the electric field can be found to change the direction of the domain, with PZT-SKN and PSKZTN shows a relatively high polarization value (P_r) shows that the transmission of electric charge. The heavens are easier to do when stimulated by external energy.

STUDY THE ELECTRICITY PRODUCTION OF THE CERAMIC TAPE THAT IS PREPARED

After the ceramic tape went through an electrical conductivity of 3 kV mm^{-1}, the piezoelectric properties could be determined from the pico-coefficient (d_{33}). PZT-SKN, and PSKZTN showed the values d_{33} highest in the group. Which is partly a result of the ions of K^{1+} that allow electric charges to move more easily When the ceramic tape was fabricated into a piezoelectric module using silver glue between the tape and brass sheet, when testing the production of oscillation, the rectifier could help to increase the voltage. Electricity from oscillation of the piezoelectric module However Piezoelectric modules are thin and easily broken when the magnitude of the force is very high. The tape piezoelectric module is therefore suitable for applications from very small mechanical energy such as vibrations, which will produce better electricity through pressures.

SUGGESTIONS

1. To prepare ceramic tapes, many types of solutions are used. Should try to reduce the amount of solution or use deionized water to aid in tape synthesis Moreover, the mixing of the solution must be homogeneous and without air bubbles, therefore requires high quality stirring tools and vacuum pumps.

2. Burning of the tape requires a high amount of time and temperature for burning, causing the tape breaking and melting to stick to the foundation easily. (Due to the thin tape) should be used as a base that is resistant to high heat. Does not cause the tape to adhere and not more than 1 mm thin, such as aluminum nitride plates

3. In the production of electricity from piezoelectric modules, it depends on the area of the tape. Therefore, the tape size should be designed to be larger in accordance with the size of the experiment set. Or suitable for the usage area in order to obtain the most power generation from the module.

REFERENCES

REFERENCES

C.Z. Rosen, B.V. Hiremath and R.E. Newnham, Piezoelectricity, New York, 1992, l p. 10- 15

D. A. van den Ende, S. E. van Kempen, X. Wu, W. A. Groen, C. A. Randall, and S. van der Zwaag, J. Appl. Phys. 2012, 111, 124107.

D. Damjancovic, N. Klein, J. Li, V. Porokhonskyy, 2010, Functional Materials Letters, 3, 5-13.

D. Hotza, P. Greil, Review: aqueous tape casting of ceramic powders, Mater. Sci. Eng. A 202 (1995) 206–217.

D. Xiao, D. Lin, J. Zhu, P. Yu, 2008, Journal of Electroceramics, 21, 34-38.

E.A. Gurdal, S.O. Ural, H.-Y. Park, S. Nahm, K. Uchino, 2011, The Japan Society of Applied Physics, 50, 027101.

E. Aksel, J.L. Jones, 2010, Sensors, 10, 1935-1954.

Fuli Zhu, Jinhao Qiu, Hongli Ji, Kongjun Zhu, and Kai Wen. (2015). Comparative investigations on dielectric properties and humidity resistance of PZT-SKN and PZT-SNN ceramics. Journal of Materials Science: Materials in Electronics, 26(5), 2897-2904

G Helke, S Seifert, and S.J. Cho. (1999). Phenomenological and Structural Properties of Piezoelectric Ceramics Based on $XPb(Zr, Ti)O_3$-$(1-x)Sr(K_{0.25}, Nb_{0.75})O_3$ (PZT/SKN) Solid Solutions. Journal of the European Ceramic Society, 19, 1265-1268.

G.N. Howatt, R.G. Breckenridge, J.M. Brownlow, Fabrication of thin ceramic sheets for capacitors, J. Am. Ceram. Soc. 30 (1947)

237–242.

G.N. Howatt, Method of Producing High Dielectric High Insulation Ceramic Plates, US Patents No. 2582993 (January 1952).

H. Li, W.-H. Shih, W.Y. Shih, 1993, Journal of the American Ceramic Society, 1852-1855

H. Nalwa, Ferroelectric polymers, New York, 1995, p. 13-15.

I. Babu and G. de. With, Composites Science and Technology. 2013; Submitted. [33] K.A. Klicker, J.V. Biggers and R.E. Newnham, J. Am. Ceram. Soc., 1982, 64:5.

J.S. Zhao, D.Y. Park, M. J. Seo, C. S. Hwang, Y. K. Han, C. H. Yang and K. Y. Oh J. Electrochem. Soc. 2004 151(5): C283-C291.

M. Rahaman, Ceramic Processing, Wiley Online Library, 2006.

M. Toyama, R. Kubo, E. Takata, K. Tanaka, K. Ohwada, Sensors and Actuators A: Physical, 1994, 45, 2, 125–129.

M. Demartin Maeder, D. Damjanovic, N. Setter, 2004, Journal of Electroceramics, 13, 385- 392.

Niall J. Donnelly, Thomas R. Shrout, and Clive A. Randall. (2007). Addition of a Sr, K, Nb (SKN) Combination to PZT(53/47) for High Strain Applications. Journal of the American Ceramic Society, 90(2) 490-495

R.E. Mistler, E.R. Twiname, Tape Casting, Theory and Practice, American Ceramic Society, 2000.

S. Abhinay, R. Mazumder, A. Seal, A. Sen. (2016). Tape casting and electrical characterization of $0.5Ba(Zr_{0.2}Ti_{0.8})O_3$-$0.5(Ba_{0.7}Ca_{0.3})TiO_3$ (BZT-0.5BCT) piezoelectric substrare. Journal of the European Ceramic Society, 36(2016) 3125-3137

S. Jeong, J. Shi-Zhao, H.R. Kim, D.Y. Park, C. S. Hwang, Y. K. Han, C. H. Yang, K. Y. Oh, S. H. Kim, D.S. Lee and J. Ha, J. Electrochem. Soc. 2003, 150, 10, C678-C687.

T. Yamada, T. Udea and T. Kitayama, J. Appl. Phys., 1982, 53, p. 4328-4332. [23]

T. Furukawa, K. Ishida and E. Fukada, J. Appl. Phys., 1979, 50, p. 4904-4912.

Wenli Zhang, and Eitel E. Richard. (2011). Low-temperture sintering and properties of 0.98PZT-0.02SKN cermics with $LiBiO_2$ and CuO addition. Journal of the American Ceramic Society, 94(10), 3386 – 3390

Wenli Zhang and Richard E. Eitel. (2013). Sintering Behavior, Properties, and Applications of Co-Fired Piezoelectric/Low Temperature Co-Fired Ceramic (PZT-SKN/LTCC) Multilayer Ceramics. Journal of Applied Ceramic Technology, 10(2) 354-364

W. D. Kingery, H. K. Bowen, and D. R. Uhlmann. Introduction to Ceramics. New York: John Wiley & Sons. (1960)

Xiaolian Chao, Lili Yang, Hong Pan, and Zupei Yang. (2012). Fabrication, temperature stability and charateristics of $Pb(Zr_xTi_y)O_3$ – $Pb(Zn_{1/3}Nb_{2/3})O_3$-$Pb(Ni_{1/3}Nb_{2/3})O_3$ piezoelectric ceramics bimorph. Ceramics International, 38,3377-3382.

Y. Sakashita, T. Ono, H. Segawa, K. Tominaga, and M. Okada, J. Appl. Phys. 1991, 69, 8352.

APPENDIX

Publication

Orapan Hemadhulin, J .Kongphimai, W .Photankham,P. Srinuanlae and H .Wattanasarn. Fabricating Piezoelectric Tape of PZT-SKN, Journal of Physics: Conf. Series 1259 (2019) 012008

Journal of Physics: Conference Series

PAPER • **OPEN ACCESS**

Fabricating Piezoelectric Tape of PZT-SKN

To cite this article: O. Hemadhulin *et al* 2019 *J. Phys.: Conf. Ser.* **1259** 012008

View the article online for updates and enhancements.

IOP ebooks™

Bringing you innovative digital publishing with leading voices to create your essential collection of books in STEM research.

Start exploring the collection - download the first chapter of every title for free.

This content was downloaded from IP address 223.206.249.34 on 17/09/2019 at 08:37

Fabricating Piezoelectric Tape of PZT-SKN

O. Hemadhulin[1], J .Kongphimai[2], W .Photankham[3],P. Srinuanlae[4] and H .Wattanasarn[5]*

[1] Faculty of Science and Technology, Sakon Nakhon Rajabhat University,
Sakon Nakhon 47000, Thailand
[2] Piezoelectric Research Laboratory, Center of Excellence on Alternative Energy, Research and Development Institution, Sakon Nakhon Rajabhat University, Sakon Nakhon 47000, Thailand

*Corresponding author .Email :w_wattanasarn@hotmail.com

Abstract. Tape ceramics are widely used in the sensor and electronic industries. In this work, we studied the ferroelectric properties of the $0.975Pb(Zr_{0.52}Ti_{0.48})O_3$-$0.025Sr(K_{0.25}Nb_{0.75})O_3$ tape ceramic; (PZT-SKN). We fabricated the PZT-SKN using doctor blade technique with the slurry, obtained from the calcined of PZT-SKN mixing with organic solution. The crystalline structure was investigated by using X-ray diffraction, relative density, and Vickers Hardness technique. We also determined the dielectric properties and polarization electric field loops. The results of crystalline structure show that the percentage of perovskite is 97.57 %, the relative density is 98.4 %, and Vickers Hardness is 107 MPa. At the thickness 0.89 mm, the dielectric constant temperature is 1499 at 532 °C, the remnant polarization is 17 $\mu C\ cm^{-2}$, Currie temperature is 552 °C, and piezoelectric coefficient is 235 $pC\ N^{-1}$. The PZT-SKN tape ceramic has the ferroelectric properties better than tablet ceramic.

Keywords :PZT-SKN; Piezoelectric tape; Tape ceramic; Fabricated; Ferroelectric

1. Introduction

Piezoelectric devices on lead zirconate titanate ceramic (PZT) base are widely used in the medical, sensor and electronic industries for exceptional piezoelectric properties. The PZT is the most widely for transducer and actuator due to its flexibility in doping materials and property design, and low cost [1,2]. The ceramic plate forming process can be assembled into electronic devices. There are many ways to use in the screen printing, calendaring and tape casting. Tape casting is another interesting which first introduced in the 1940s [2–4]. In tape casting, the slurry is spread over a surface using the doctor-blade process. The doctor-blade process can be controlled a thickness film from 1 μm up to 3000 μm [4–10]. In addition, the ceramic materials are favor application in the electrical equipment. The Sr^{+2}, K^{+1}, and Nb^{+5} doped PZT (PZT-SKN) has been studied for multilayer actuators and transducers [11]. The ratio of Zr/Ti in the PZT-SKN ceramics with formula 0.98PZT-0.02SKN has been studied in morphotropic phase transition. Rhombohedral and tetragonal crystal structure show coexist at 300 °C in the Zr/Ti range of 55/45 to 52/48 [12]. In addition, the PZT-SKN ceramics show high piezoelectric coefficient and permittivity values with a high Curie temperature, which is good thermal stability.

In this work, $0.975Pb(Zr_{0.52}Ti_{0.48})O_3$-$0.025Sr(K_{0.25}Nb_{0.75})O_3$; (PZT-SKN) was fabricated using tape casting technique with doctor blade contorted tape ceramic thickness. The crystal structure was studied by X–ray diffraction technique (XRD). The physical properties were determined by relative density and Vickers Hardness technique. Ferroelectric properties were investigated by dielectric properties, polarization electric field loop, and the piezoelectric coefficient (d_{33}).

Content from this work may be used under the terms of the Creative Commons Attribution 3.0 licence. Any further distribution of this work must maintain attribution to the author(s) and the title of the work, journal citation and DOI.
Published under licence by IOP Publishing Ltd

2 .Materials and Methods

The PZT-SKN powder was prepared by solid state route. Reagent grade of powder lead oxide (PbO, 99.00%) titanium dioxide (TiO_2, 99.00%) strontium carbonate oxide ($SrCO_3$, 99.00%) potassium carbonate (K_2CO_3, 99.00%) and niobium oxide (Nb_2O_5, 99.00%) were used as the precursor materials. A stoichiometric amount of powders was mixed by a bally for 24 h with zirconia ball using deionized water as media. The mixture was dried at 100 °C overnight in an oven. The mixture was placed in a crucible, which was subsequently inserted into the furnace in the calcine burnt at a temperature of 850 °C for 4h.

Typical PZT-SKN slurry was made as per the composition given in Table 1. The preparation of slurry for tape casting was carried out in two stages. In the first phase, mixture of methyl ethyl ketone (MEK), ethanol and phosphate ester hey were ball milled for 24 h in polyethylene jar using ZrO2 balls as grinding media. and in the second stage binding system consisted of binder (polyvinyl butyral, PVB) and plasticizers (polyethylene glycol, PEG). In both the cases, they were ball milled for 6 h in polyethylene jar using ZrO2 balls as grinding media. After mixing by ball milling, wire mesh filter slurry, then vacuum the pump out with a vacuum pump (Ax–2000 Vacuum Mixer). Then the slurry was cast in a laboratory tape caster with the stationary reservoir. A casting speed of 1.20 mms/s was maintained in all cases and left for drying. Square dimensional sample (2×2 cm^2) were cut from the green tapes. Then bake at a temperature of 100–200 °C for 1 h., leave to room temperature. Then burn binder with a temperature of 350–750 °C. leave it for 2 hours and leave to room temperature. The final sintering using the sintering temperature of 1100 ° C, the temperature dropped to room temperature for 2 h. and then leave. After examining the dielectric properties of 1–100 kHz and temperature range 30–600 ° C, examination of Ferroelectric Properties by study of hysteresis loop, the polling at room temperature for 10 min using a voltage of 2.5 kV mm^{-1} and measurement of piezoelectric coefficient.

มหาวิทยาลัยราชภัฏมหาสารคาม

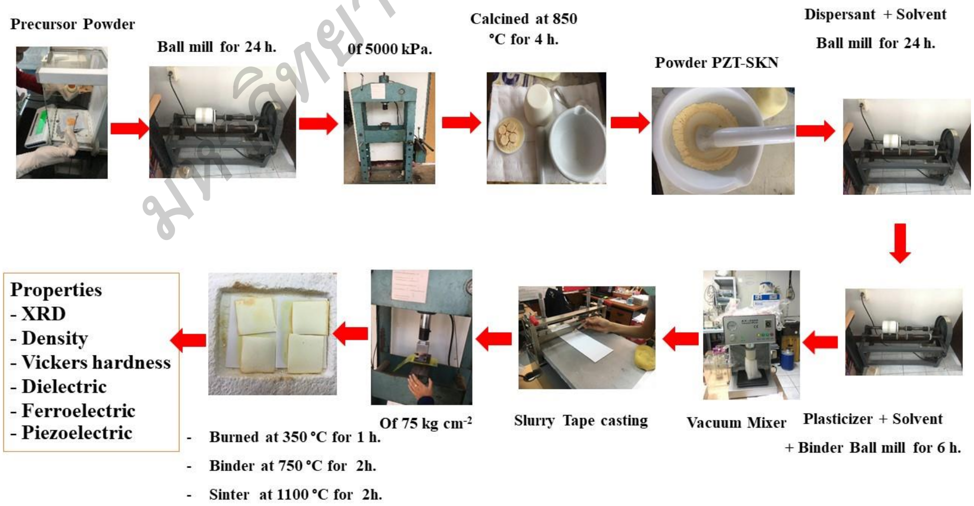
Precursor Powder
Ball mill for 24 h.
Of 5000 kPa.
Calcined at 850 °C for 4 h.
Powder PZT-SKN
Dispersant + Solvent
Ball mill for 24 h.
Properties
- XRD
- Density
- Vickers hardness
- Dielectric
- Ferroelectric
- Piezoelectric
- Burned at 350 °C for 1 h.
- Binder at 750 °C for 2h.
- Sinter at 1100 °C for 2h.
Of 75 kg cm^{-2}
Slurry Tape casting
Vacuum Mixer
Plasticizer + Solvent
+ Binder Ball mill for 6 h.

Figure 1. The experimental schematic.

Table 1 Composition of the PZT-SKN tape casting slurry.

Ingredient	Function	Weight (%)
Powder	Ceramic	65
Phosphate Ester	Dispersant	1
Methyl Ethyl Ketone +Ethanol	Solvent	26
Polyvinyl Butyral	Binder	4
Polyethylene Glycol	Plasticizer	3

3 .Results and Discussion

The XRD patterns of the (1 –x)PZT-xSKN sintered at 1100 °C are illustrated in Figure 2. Our result revealed that the Zr/Ti ratio is 52/48 in a tetragonal structure with lattice parameters a = b=4.036 Å, c = 4.146 Å. The crystalline structure of the tape PZT ceramic had a tendency to change from tetragonal to rhombohedral structure [4–7] when added SKN. It is noticeable that the (002) and (200) peaks spited into two peaks [4]. Therefore, it is confirmed that the crystal structure of the PZT tape ceramic has changed by SKN. The density with value of 6.0353 g cm^{-3} combined with the theoretical density with value of 6.13 g cm^{-3} yielded the relative density value of 98.4 %. The measured Vickers hardness is 107 MPa.

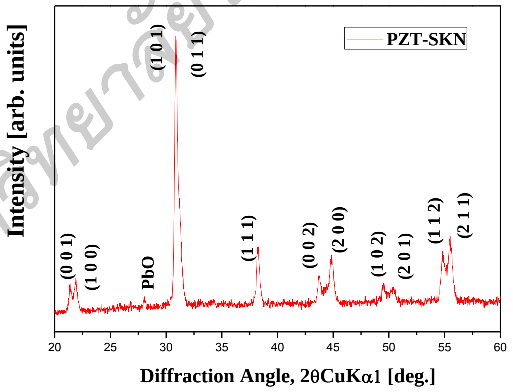

Figure 2. The illustrated of XRD pattern of tape PZT-SKN ceramic.

The Figure 3 shows dielectric constant and dielectric loss of the tape PZT-SKN ceramic at temperature range 30– 600°C and frequency range 1 – 100kHz, respectively. The results showed that the dielectric constant maximum ε_r is 1499 at 532 °C and 1 kHz. Similarly, dielectric losses became reduced at 32 °C and 1 kHz with tanδ value of 0.154. It is contributed to high dielectric properties. The temperature at which this spike occurs is the Curie point, T_0. Above this temperature, the permittivity decreases according to the Curie-Weiss Law the inverse of permittivity versus temperature should provide a linear relationship past the Curie point if the Curie-Weiss Law is followed. The slope of this line will equal the inverse of the Curie constant and the y-intercept will equal T_C, the Curie temperature, divided by the Curie constant. An example plot, fitting, and calculated values are shown in Figure

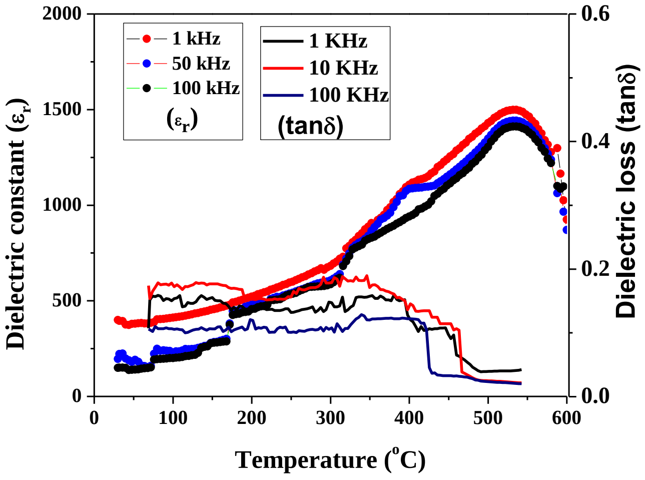

Figure 3. The relative dielectric constant and dielectric loss of the tape PZT-SKN ceramic.

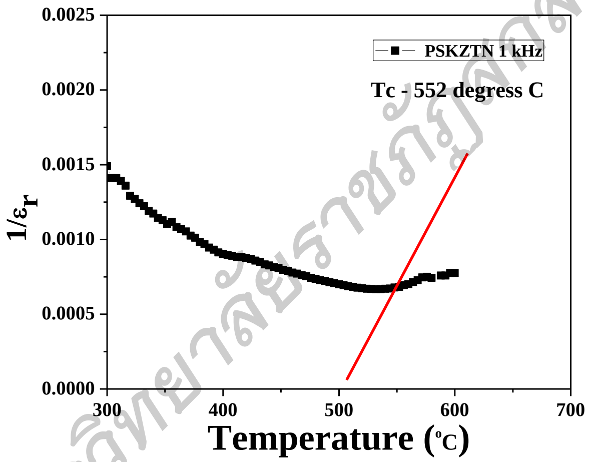

Figure 4. The Currie constants and temperatures for the tape PZT-SKN ceramic.

From checking the polarization of the PZT-SKN showed the characteristics of piezoelectric the soft type is a characteristic of a hard piezoelectric. Because the squareness loop, indicating that it uses more energy [20–25]. Figure 5 the results measured the polarization and hysteresis loop of the tape PZT-SKN ceramic at thickness 0.89 mm, the coercive field at 3 kV mm^{-1} and 4 kV mm^{-1}. It was found that the 3 kV mm^{-1} coercive field had $P_r \approx 17$ µC cm^{-2} and $E_c \approx 20$ kV cm^{-1}, the coercive field is 4 kV mm^{-1} with $P_r \approx 20$ µC cm^{-2} and $E_c \approx 25$ kV cm^{-1}. This shows that when there is an increase in coercive field passed on to the polarization hysteresis loops of tape PZT-SKN ceramics is increased. When the tape PZT-SKN ceramic electrodes to induce an electric field under a voltage 2.5 kV mm^{-1} and a temperature of 150 °C at 15–30 minutes. When the workpiece through the inductor electrodes to measure the piezoelectric coefficient found that piezoelectric coefficient is 235 pC mm^{-2}.

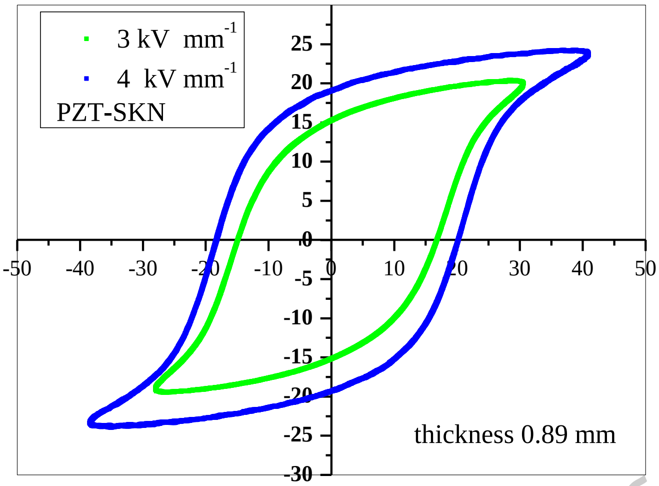

Figure 5. Room temperature P–E hysteresis loops of the tape PZT-SKN ceramic.

4. Conclusion

The tape PZT-SKN ceramic were synthesized by tape casting method sintering at 1100 °C at 2 h. The XRD patterns of the PZT-SKN show the trend of crystal structure change from tetragonal to the rhombohedral. It is noticeable that the plane (002) and (200) [1, 5]. The measurement density and Vickers hardness, density 6.0353 g cm^{-3}, theoretical density was 6.13 g cm^{-3}, it has a relative density of 98.4% and a Vickers hardness of 107 N mm^{-2}. The dielectric constant and dielectric loss, ε_r = 1499 of temperature 532 °C at a frequency of 1 kHz, tanδ = 0.154 at 32 °C with a frequency of 1 kHz. The P–E hysteresis loops at 4 kV mm^{-1} with $P_r \approx 20$ μC cm^{-2} and $E_c \approx 25$ kV cm^{-1} and piezoelectric coefficient 235 pC mm^{-2}. The study properties of ceramic tape PZT-SKN found that such material is applied to a capacitor in a small electronic circuit.

Reference

[1] Cross L E and Newnham R E. Hight-Technology Ceramics: Past, Present, and Future – The Nature of Innovation and Change in Ceramic Technology. (1986) 289–305

[2] Howatt G N, Breckenridge R G, Brownlow J M, Fabrication of thin ceramic sheets for capactions. *Journal of the American Ceramic Society*, 30 (1947) 237–142

[3] Hotza D, Greil P, Review: aqueous tape casting of ceramic powders. Mater. Sci Eng. A 202 (1995) 206–217

[4] Fuli Zhu, Jinhao Qiu, et al, Comparative investigations on dielectric properties and humidity resistance of PZT–SKN and PZT–SNN ceramics. *Journal of Materials Science: Materials in Electronics*, **26(5)**, 2897–2904 (2015).

[5] G Helke, S Seifert, and S.J .Cho, Phenomenological and Structural Properties of Piezoelectric Ceramics Based on XPb)Zr, Ti(O_3–)1–x(Sr)$K_{0.25}$, $Nb_{0.75}$(O_3) PZT/SKN (Solid Solutions . *Journal of the European Ceramic Society*, **19**, 1265–1268) 1999.

[6] Niall J .Donnelly, Thomas R .Shrout, and Clive A .Randall, Addition of a Sr, K, Nb)SKN (Combination to PZT) 53/47 (for High Strain Applications .*Journal of the American Ceramic Society*, **90)2(**, 490–495)2007.

[7] Wenli Zhang, and Eitel E. Richard, Low-temperture sintering and properties of 0.98PZT-0.02SKN ceramics with $LiBiO_2$ and CuO addition. *Journal of the American Ceramic Society*, **94(10)**, 3386–3390 (2011).

[8] Jukkrit Kongphimai, Wattana Photankham, et all, Effect of Sb2O3 Doping Pb)$Zr_{0.53}Ti_{0.47}$(O_3 Ceramics .*Journal of Materials Science and Applied Energy*, **6)3(**, 226–229) 2017

[9] Wattanasarn H, Kongphimai J, et all, Dielectric and ferroelectric properties of Pb)$Fe_{1/2}Nb_{1/2}$(O_3 modification on Pb)$Zr_{0.52}Ti_{0.48}$(O_3 ceramics .*Integrated Ferroelectrics*, **187:1**, 89–99) 2018.

[10] Photankham W, Kongpimai J, et all, Effect of PFN addition on microstructure and piezoelectric properties of PZT58/42 ceramics .*Integrated Ferroelectrics*, **187:1**, 80–88) 2018.

[11] Wattanasarn H, Kongpimai J, et all, Effect of ZnO addition on ferroelectric properties of $0.94PbFe_{1/2}Nb_{1/2}$(O_3– $0.06PbTiO_3$ and 0.9Pb)$Fe_{1/2}Nb_{1/2}$(O_3–$0.1PbTiO_3$ ceramics .*Integrated Ferroelectrics*, **187:1**, 33–44) 2018.

[12] Wenli Zhang and Richard E. Eitel, Sintering Behavior, Properties, and Applications of Co−Fired Piezoelectric/Low Temperature Co−Fired Ceramic (PZT−SKN/LTCC) Multilayer Ceramics. *Journal of Applied Ceramic Technology*, **10(2)**, 354–364 (2013).

[13] Xiaolian Chao, Lili Yang, et al, Fabrication, temperature stability and characteristics of $Pb(Zr_xTi_y)O_3 – Pb(Zn_{1/3} Nb_{2/3})O_3–Pb(Ni_{1/3}Nb_{2/3})O_3$ piezoelectric ceramics bimorph. *Ceramics International*, **38**, 3377−3382 (2012).

[14] Hong Liun, Rui Nie, et all, Effect of MnO_2 doping on piezoelectric, dielectric and ferroelectric properties of PNN–PZT ceramics. *Ceramics International*, **41**, 11359−11364 (2015).

[15] Divya A S, Juairiya P, et all, Influence of A−site Sr^{2+} substitution on structure, dielectric and ferroelectric characteristics of $0.66[Pb(In_{0.50}Nb_{0.50})O_3]–0.34[PbTiO_3]$. *Ceramics International*, **43**, 825–829 (2017).

[16] Alexander V. Petrov, Jan Macutkevic, Synthesis and dielectric properties of ferroelectric-ferrimagnetic PZT−SFMO composites. *Modern Electronic Materials 3*, 26–31 (2017).

[17] Shara Sowmya N, Srinivas A, Studies on magnetoelectric coupling in lead-free [(0.5) BCT−(0.5) BZT]−$NiFe_2O_4$ laminated composites at low and EMR frequencies. *Journal of Alloys and Compounds*, **743**, 240–248 (2018).

[18 Chandrakala E, Paul Praveen J, et a, Effect of sintering temperature on structural, dielectric, piezoelectric and ferroelectric properties of sol–gel derived BZT−BCT ceramics. *Ceramics International*, 42, 4964–4977 (2016).

[19] Divya AS and Kumar V, Influence of Fe^{3+} substitution on the dielectric and ferroelectric characteristics of Lead Indium Niobate. *Journal of Alloys and Compounds*, **637**, 426–430 (2015).

[20] Corredores a Y, Le Febvrier A, et a, Study of ferroelectric/dielectric multilayers for tunable stub resonator applications at microwaves. *Thin Solid Films*, **553**, 109–113 (2014).

[21] Parveen Kumar, Juneja J K, et all, Effect of Sm on dielectric, ferroelectric and piezoelectric properties of BPTNZ system. *Physica B*, **426** 112–117 (2013).

[22] Aditya Jain, Amrish K. Panwar, et al, Improvement in dielectric, ferroelectric and ferromagnetic characteristics of $Ba_{0.9}Sr_{0.1}Zr_{0.1}Ti_{0.9}O_3–NiFe_2O_4$ composites. *Ceramics International*, **43**, 10253–10262 (2017).

[23] Zhenzhen Song, Yongcheng Zhang, et al, Fabrication and ferroelectric/dielectric properties of La−doped PMN−PT ceramics with high optical transmittance. *Ceramics International*, **43**, 3720–3725 (2017).

[24] Siripong Somwan a, Athipong Ngamjarurojana, et a, Dielectric, ferroelectric and induced strain behavior of PLZT 9/65/35 ceramics modified by Bi2O3 and CuO co−doping. *Ceramics International*, **42**, 10690–10696 (2016).

[25] Abhinay S, Mazumder R, Seal A, Sen A, Tape casting and electrical characterization of 0.5Ba)$Zr_{0.2}$ $Ti_{0.8}$(O_3-0.5)$Ba_{0.7}Ca_{0.3}$(TiO_3)BZT−0.5BCT (piezoelectric substrate .*Journal of the European Ceramic Society*, **36**, 3125–3137)2016.

CURRICULUM VITAE

CURRICULUM VITAE OF RESEARCHER

Name		Orapan Hemadhulin
Data of birth		11 November 1992
Current location		164 Moo 3, Kham Bo Subdistrict, Waritchaphum District, Sakhonnakon Province, 47150, Thailand
E-mail:		Oh.hemadhulin139@gmail.com
History of education		
	2002	4th year Primary 1-4, Tat Phu wong School, Kham Bo Subdistrict, Waritchaphum District, Sakhonnakon Province, 47150, Thailand
	2004	2nd year Primary 5-6, Banhiplalo School, Plalo Subdistrict Waritchaphum District, Sakhonnakon Province, 47150, Thailand
	2010	6th year High school, Matthayomwaritchaphum School, Plalo Subdistrict, Waricthaphum District, Sakon Nakhon, Thailand
	2016	Bachelor of Education in Science (Physics), Loei Rajabhat University